REPORT DOCUMENTATION PAGE

Form Approved OMB No. 0704-0188

1. AGENCY USE ONLY (Leave blank)	2. REPORT DATE	3. REPORT TYPE AND DATES COVERED
	May 2000	Final Report

4. TITLE AND SUBTITLE

Advanced Mixing of Fuel/Oxidant System in High Speed Gaseous Flows Stage I

5. FUNDING NUMBERS

F61775-99-WE093

6. AUTHOR(S)

Dr. Valentin Bityurin

7. PERFORMING ORGANIZATION NAME(S) AND ADDRESS(ES)

Russian Academy of Sciences
IVTAN, Izhorskaya str., 13/19
Moscow 127412
Russia

8. PERFORMING ORGANIZATION REPORT NUMBER

N/A

9. SPONSORING/MONITORING AGENCY NAME(S) AND ADDRESS(ES)

EOARD
PSC 802 BOX 14
FPO 09499-0200

10. SPONSORING/MONITORING AGENCY REPORT NUMBER

SPC 99-4093

11. SUPPLEMENTARY NOTES

Report on CD.

12a. DISTRIBUTION/AVAILABILITY STATEMENT

Approved for public release; distribution is unlimited.

12b. DISTRIBUTION CODE

A

13. ABSTRACT (Maximum 200 words)

This report results from a contract tasking Russian Academy of Sciences as follows: The proposed advanced mixing approach is to increase the reacting volume growth for mixing enhancement by (1) pulse electrical discharge and (2) by MHD interaction. The task of this activity is to develop an integrated model including all significant mechanisms of in-flow mixing and controlling means. Such a model can be used to formulate an experimental program on the validation of proposed principles. The following deliverables are anticipated: 1) Feasibility study and prospective assessments; 2) Development of sophisticated physical and numerical models of fuel/oxidant kinematics mixing under active MHD & Plasma affects; 3) Parametric studies for ram/scramjet applications; 4) Preliminary experimental validation proposal; 5) Reporting.

14. SUBJECT TERMS

EOARD, Fuels, Mixing

15. NUMBER OF PAGES

241

16. PRICE CODE

N/A

17. SECURITY CLASSIFICATION OF REPORT	18. SECURITY CLASSIFICATION OF THIS PAGE	19. SECURITY CLASSIFICATION OF ABSTRACT	20. LIMITATION OF ABSTRACT
UNCLASSIFIED	UNCLASSIFIED	UNCLASSIFIED	UL

Final Report
on

EOARD Contract SPC 99-4093

Advanced Mixing of Fuel/Oxidant System in High Speed Gaseous Flows Stage I.

Delivery 3.

Principal Investigator
V.A.BITYURIN , PhD, DS
Institute of High Temperatures
Russian Academy of Sciences

May 2000
Moscow

Contents

I. Introduction

The process of mixing of gaseous fuel and oxidant is one of fundamental subjects of combustion and propulsion research. It is basically clear that the better (faster) mixing the higher combustion efficiency can be reached under similar conditions. The mixing can be critically important for short residence time combustion systems such as scramjet.

The theory of combustion in so-called premixed systems is developed for a long time [1-3]. The key question in such a system is the flame propagation.

Two different modes of the flame propagation are usually considered: laminar and turbulent. The laminar process of combustion is defined by balance of heat release in the flame front due to chemical reactions between fuel and oxidant and energy transfer by heat conductivity.

In the case of turbulent combustion the effective flame propagation velocity increases significantly due to important role of convection in energy transport from the heat release region to the undisturbed flammable mixture. In fact the turbulence in the combustion zone can be created due to intensive heat release (heating resulting in non-steady state expansion flow of gaseous products and fresh mixture) or/and it can be convected by the flow to the combustion zone as well [3].

In contemporary combustion systems such as combustion chamber of (turbo)jets, ramjet, scramjet combustion starts in only partially mixed flow where the fuel/oxidant ratio varies significantly in working volume. In this particular but very important practical case the combustion and mixing can develop simultaneously affecting each other [4-6] (see also [7] with many example of particular recently performed studies in the field). The combustion as an elementary chemical reaction between fuel and oxidant molecules needs the direct contact (collision) of these molecules. Thus, the combustion can occur if in a particular location the collision between fuel and oxidant molecule can take place. This «molecular» level of mixing is provided by conventional molecular diffusion. However, the molecular diffusion is generally speaking very slow process in scale of available mixing time, which is limited, by residence time in combustion zone. To enhance the mixing process the other «large scale» mechanism of mixing is introduced. The main idea is to increase the contact surface between fuel and oxidant. The simplest well-known method is rotating mixing widely used in mankind practice for whole human history. The turbulence motion is basically a vortex motion and one can consider the turbulence enhancement of mixing as a combined effect of different scale rotating mixing cells. This, *kinematics,* stage of mixing increases the all inter-component contact surfaces. (The theory of kinematics mixing based on a Lagrangian' non-turbulence approach is recently presented in a textbook by J.M.Ottino [8]. The kinematics

treatment of the turbulence for the mixing study is independently proposed and developed in our recent papers [9-12].)

Simultaneously the conventional molecular diffusion across the contact surface develops providing the mutual penetration of fuel into the oxidant fluid domain and, the oxidant, to the fuel fluid domain. As a result at the contact fuel and oxidant domain a intermediate diffusion region is formed where the fuel-to-oxidant ratio varies between its limits 0 and ∞. The characteristics thickness of such a layer is estimated by

$$\delta \approx \sqrt{Dt}$$

where D and t are diffusion coefficient and time of the contact, correspondingly.

Thus, increasing contact surface and diffusions layer forms a *reacting volume* where the combustion can occur.

The concept of the reacting volume has been formulated by us in series of papers dealing with the evolution of plasma clots in a channel flow [9-11], and more recently to treat the current break-off in a gaseous current breaker device [12]. In these studies the reacting volume evolution was described with taking into account of the turbulence flow field. Furthermore, the turbulence is considered as flow characteristics modified by electromotive body force $\mathbf{j}\times\mathbf{B}$. The important feature of the body force is its vortex nature.

This concept was rather fruitful and, for this reason, it was proposed to check a similar approach to analysis of non-premixed combustion in supersonic flows with enhanced turbulence by electromotive body force $\mathbf{j}\times\mathbf{B}$.

The objective of the present work is (1) to check the reacting volume concept for combustion study applications; (2) to adopt the numerical models developed for gas-plasma flows analysis for the combustion conditions; (3) to develop the numerical model of combustion under high-speed flow conditions with MHD interaction assisted fuel-oxidant mixing.

II. Kinematics of mixing in fluids

Presently, the study of fluid mixing has very little scientific basis; processes and phenomena are analyzed on a case-by-case basis without any attempt to discover generality. For example, the analysis of mixing and 'stirring' of contaminants and tracers in two-dimensional geophysical flows such as in oceans; the mixing in shear flows and wakes relevant to aeronautics and combustion; the mixing of fluids under Stokes's regime generally encountered in 'blending' of viscous liquids such as polymers; and the mixing of diffusing and reacting fluids encountered in various types of chemical reactors share little in common with each other, except possibly the nearly universal recognition among researchers that they are very difficult problems.

There are, however, real similarities among the various problems and the possible benefit from overall attack on the problem of mixing using a general viewpoint are substantial. The contribution of the present very particular efforts can be useful in the field of constructing of practical evaluation procedures, which can provide more direct references to the experimental data, and, in turn, development advanced mixing technique.

The point of view adopted in this study based on two main ideas.

The first one seems to be fully similar to the formulated by J.Ottino in his book [8] is that from kinematics viewpoint fluid mixing is the efficient stretching and folding of material lines and surfaces. Such a problem corresponds to the solution of the dynamical systems

$$dx/dt = v(x,t)$$

with $x = X$ at time $t=0$.

The solution of the above system $x=\Phi_t(X)$ is called *the flow motion* in the approach of the book[8]. It is explained there that even in the simplest cases this "solution" might be extremely hard to obtain. The kinematical foundations lie in an understanding of the point transformation $x=\Phi_t(X)$.

In the frame of such an approach the following three sub-programs are considered:

(1) Mixing of s single fluid or similar fluids.

The basic objective here is to compute the length (of area) corresponding to a set of initial conditions. As it can be shown (see, for example, [8]) only in few cases it can be done exactly and in most of these the length is mild. The best achievable mixing corresponds to exponential stretching nearly everywhere and occurs in some regions of chaotic flows.

It should be noted also that the latter case was considered in our papers [9-13] as main mechanism of the mixing in turbulent flows with the reference to Batchelor's hypothesis of exponential stretching law.

However, under these conditions the (exact) calculation of the length and location of lines and areas is hopelessly complicated. As it is shown in [8] even extremely simplified flows might be inherently chaotic and a complete characterization is not possible. For example, from a dynamical systems viewpoint if the system possesses horseshoes infinitely many periodic points occurred all of which cannot be calculated precisely. Fortunately, as far as mixing is concerned the low periodic events are of interest, since the quick mixing is desirable. Nevertheless, there is always the intrinsic limitation of being unable to calculate precise information (most practical problems involve stretching of order 10^4 or higher) such as length stretch and location of material surface. This is true even though none of the flows discussed in [8] is turbulent in an Eulerian sense. Rather, the previous finding should be used to establish the limits of what might constitute reasonable answer in more complicated flows (real turbulent flows come immediately to mind). *The problem here how to best characterize the mixing, knowing beforehand that a complete characterization is impossible* [8]. Furthermore, the practical goal is not only to characterize the mixing but also rather to control the mixing! So the practical approach developed in this project involves *the second idea* of *reacting volume* which will be described later.

(2) Within a framework of a family flows $x_s=\Phi_{st}(X)$, $s = 1,\ldots N;$ each of motions is assumed to be topological (see Section 2.3 of [8]); mixing of similar diffusing and reacting fluids.

This case corresponds to the case of mixing of two streams, composed of possible several species that are rheologically identical; i.e. they have the same density, viscosity, etc., and have no interfacial tension. Concurrently with the mechanical mixing there is mass diffusion, and, possible, chemical reaction. However, for simplicity, it is typically assumed that neither the diffusion nor the reaction affects the fluid motion. This case is discussed in detailed in [8] as *a lamellar structures* case.

Again, the implementation of such a kinematics approach to the particular problems considered in the project needs an accounting in some way of back affects of the "non-linear" mixing

consequences on the flow field (fluid motion). Furthermore, some kind of controllable back affects can be utilized in principle as an intensification of mixing – main goal of he present efforts.

(3) Mixing of different fluids; case in which the motions are non-topological, i.e., there is breakup and/or fusion of material elements.

In this case, the mixing of two or more fluids leads to breakup and coalescence of material regions. This problem is complicated and only few special cases belonging to this category are discussed in [8].

In Fig.1 through 5 several illustrations of the kinematics mixing are presented to be compared later with our simulation results obtained in course of the gas-plasma flow studies.

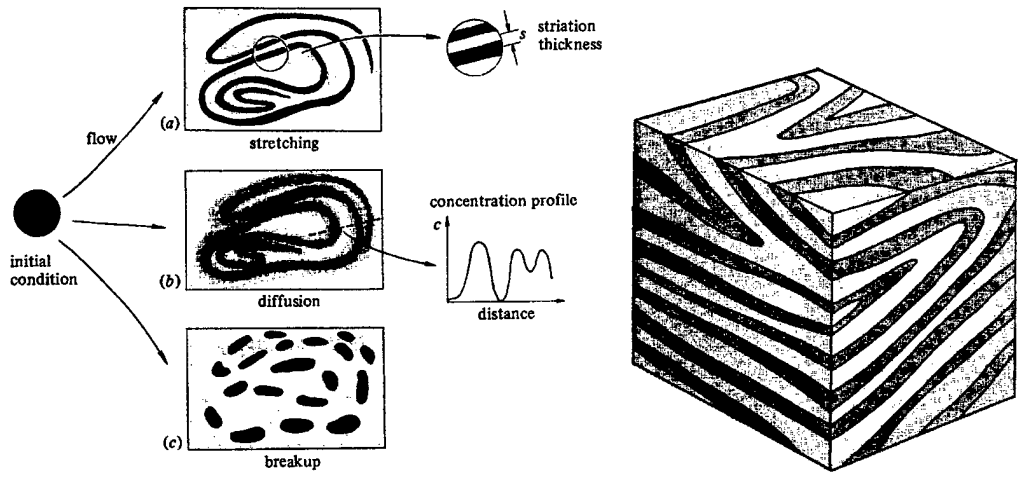

Fig.1. Basic processes occurring during mixing: (a) corresponds to the case of two similar fluids with negligible interfacial tension and negligible inter-diffusion: an initially designated material region stretches and folds by the action of a flow; (b) corresponds to a blob diffusing in the fluid: in this case the boundaries become diffuse and the extent of the mixing is given by level curves of concentrations (a profile normal to the striations is shown at the right); in (c) the blob breaks due to interfacial tension forces, producing smaller fragments which might in turn stretch and break producing smaller fragments. Case (b) is an excellent approximation to (a) if diffusion is small during the time of the stretching and folding. In (a) the blob is passive, in (c) the blob is active.

Fig.2. Growth of a "material line" composed of small hydrogen bubbles produced by a platinum wire stretched across an decaving turbulent flow behind a grid placed at the extreme left. The Reynolds number based on the wire diameter is 1.360. (Reproduced with permission from Corrsin and Karweit (1969).)

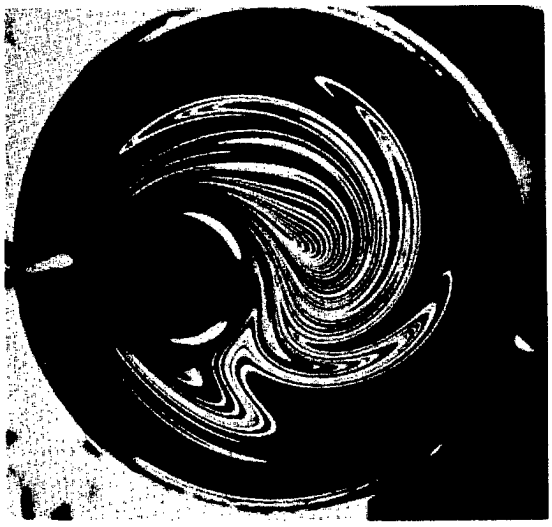

Fig.3. Mixing in a creeping flow. The figure shows the deformation of a material region in a journal bearing flow when it operates in a time-periodic fashion (experiment from Chaiken et.al. (1986)).

Fig.4. Concentration of a turbulent round jet into water at Reynolds number 2.300, measured by laser induced fluorescence; the cut is along a plane including the axis of a symmetry of the jet. (Reproduced with permission from Dimotakis, Miake-Lye, and Papantonionu (1983).)

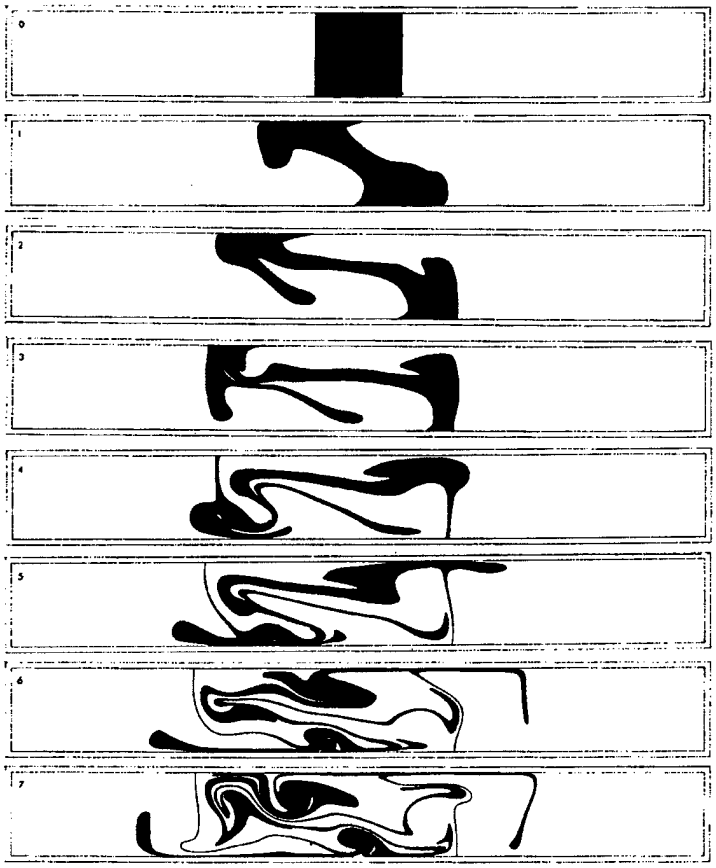

Fig.5. Deformation of a tracer in a numerical experiment of motion in the Earth mantle. The sides of the rectangle are insulating but the bottom is subjected to a constant heat flux while the temperature of the top surface is kept constant. The motion is produced by buoyancy and interval heating elects (the fluid is heated half from below and half from within). The Rayleigh number is 1.4×10^6, the time scale of the numerical simulation corresponds to 155 Myear, and the thickness off the layer is 700km. An instantaneous picture of the streamlines reveals five cells. (Reproduced with permission from Hoffman and McKenzie (1985).)

III. Gas-Plasma Flow Examples

On a Current Carrying Plasma Clot Evolution in Turbulent Flow [11-12]

Current carrying clot created in high velocity flow in an MHD channel is influenced by many factors. Energy balance of the clot is mainly defined by Joule dissipation inside the clot and energy losses trough its borders. The analyses of the current carrying clot energy balance in turbulent flow performed in our papers [11-12] has shown that the short lifetime features of the clots are strongly important for the clot evolution. It was found also that the clot temperature evolution depends on the initial shape and turbulence parameters of the flow. Three different type of clot temperature evolution were described. The electrode wall losses and the non-potential body force **j**×**B** are found to be very important as well.

1. Turbulent deformation of plasma clot.

The evolution of the initially compact volume of fluid V_m limited by surface S in the flow of incompressible fluid with uniform isotropic turbulence has been discussed in Ref[9].

Namely, it was shown in Ref.[9] that the surface growing is defined by the relation

$$S(t) = S_0 \exp\left\{\frac{1}{u} t \int_0^\infty kE(k)\, dk\right\} \qquad (1)$$

In this way surface seems to depend on time by exponent, and this is in accordance with Ref [14] For evaluation of factor in the exponent power one should take E(k) from Kolmogorov's spectrum (see, for example Ref[15,16]:

$$E(k) = \varepsilon^{2/3} k^{-5/3}$$

where ε is turbulent energy dissipation $\varepsilon \sim v^3/l$, v is basic scale of fluctuation velocity, l is basic scale of turbulence [17]. Integrating in (1) we get:

$$S(t) = S_0 \exp\left\{\frac{1}{u} \cdot t\varepsilon^{2/3} \int_{k_{\min}}^{k_{\max}} k^{-2/3} dk\right\} \qquad (2)$$

Taking instead of $k_{\max}$ following to Ref.[17] $(\mathrm{Re}/\mathrm{Re}_{\mathrm{crit}})^{3/4}/l$ (Re is Reynolds number of the basic motion and $\mathrm{Re}_{\mathrm{crit}}$ is Reynolds number of transmit from laminar to turbulent motion), instead of $k_{\min}$ $1/l$ and considered that $(\mathrm{Re}/\mathrm{Re}_{\mathrm{crit}})^{3/4} >> 1$ we get finally:

$$S = S_0 \exp\left\{\frac{v^2 (\mathrm{Re}/\mathrm{Re}_{crit})^{1/4} t}{ul}\right\} \qquad (3)$$

It is obvious, that in this kind formulas relations between values u, v and l are define with some uncertainty. For this reason some factor of order of 1 would be included in the power of exponent and from the other hand factors ~ 1 in pre-exponent expression can be canceled in this estimation.

Thus, the relation (2) should be used in practice in the form:

$$S = S_0 \exp\left\{\frac{Av^2 (\mathrm{Re}/\mathrm{Re}_{crit})^{1/4} t}{ul}\right\}$$

where factor A should be chosen by comparing with experimental data.

It is easy to see, that the turbulence «accelerates» any processes, concerned with fluxes of mass, momentum and energy (heat transfer, diffusion and so on) between volume V_{m} and ambient fluid turbulence by means this kind of the surface increasing.

Note also, that one can estimate contribution of any scale of turbulent motion in increasing of the surface to take in formula (3) integration limits k_1 and k_2, with $\Delta k = k_1 - k_2$ of order k_1:

$$S(t) = S_0 \exp\left\{\frac{t\varepsilon^{2/3} k_1^{1/3}}{u}\right\}$$

Furthermore the turbulent diffusion D_λ can be also evaluated by using this fact. It depends mainly on maximal scale, that for given time t take part in the surface deformation (for example

which increase initial surface in ε times), i.e. $D_\lambda \sim \lambda_1 v_1$, where $\lambda_1 \sim 1/k_1$ and v_1 fluctuation velocity for scale λ_1. For sufficiently large time t we get well-known formula: $D \sim lv$, because of $k_{min} \sim 1/l$.

2. Energy Effects of Turbulence

In this section evaluation of the effect of turbulence on the energy state inside a current carrying clot will be obtained when current passed through it.

A compact clot in incompressible fluid volume $V_m = \delta \times l_1 \times l_2$ with length l1 approximately equal to cross section perimeter l3 is considered. It is assume that the clot created in the flow is uniform at the initial time moment $t=0$ with constant temperature $T_0 >> T_c$ where T_c is ambient temperature. The electrical power is supplied to the clot by constant electromotive force E power source schematically shown in Fig.6.

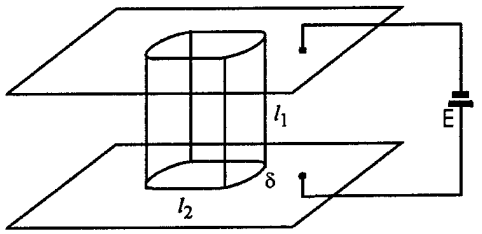

Fig.6. Schematic discharge structure in channel flow.

During the process of motion turbulence results in the clot deformation to some layers with the thickness $\delta(t)$ and the side surface of clot $S(t)$. Time dependence for $S(t)$ from (3):

$$S(t) = S_0 \exp\{\Omega t\},$$

where Ω is characteristic frequency of surface deformation development and in terms of Section 1:

$$\Omega = \frac{\nu^2}{u\lambda}(\mathrm{Re}/\mathrm{Re}_{crit})^{1/4} \qquad (4)$$

By virtue of the clot volume resistance estimation from [11] the Joule dissipation value reads:

$$q = \frac{\sigma_0(T)E_0^2 S_0}{S(t)} = \sigma_0(T)E_0^2 \exp\{-\Omega t\} \qquad (5)$$

In respect to diffusion the whole region considered can be divided in three sub regions. The first is the region of cold surrounded gas, the second is the region occupied by the clot fraction being not affected by diffusion, and the third is the mixing region with width $l_D \sim \sqrt{Dt}$. Width of this region changes in time according to said above.

In this way the equation of energy is the following:

$$\rho C_p \frac{\partial T}{\partial t} = q - \lambda_T \nabla^2 T \qquad (6)$$

Using (5), the dependence of conductivity on temperature from [18]:

$$\sigma(T) = \sigma_0 \exp\left\{m\left(\frac{1}{T_0} - \frac{1}{T}\right)\right\},$$

and evaluating ∇T as T/l_D where T is the clot temperature, the equation (6) can be presented in the form

$$\frac{\partial \theta}{\partial \tau} = B\exp\{m(1 - 1/\theta) - \tau\} - \lambda_T \frac{\theta}{l_D^2 \rho C_p \Omega} f_D, \qquad (7)$$

where

$$f_D = \begin{cases} 1, & \delta \le l_D \\ 0, & \delta > l_D \end{cases}.$$

Here new variables $\theta = T/T_0$ and $\tau = t\Omega$ and new designation

$$B = \frac{\sigma_0 E_0^2}{\rho C_p \Omega T_0} \tag{8}$$

Following [11,12] one obtains for the small values of τ

$$\theta(\tau) = \frac{B}{mB-1}\exp\{(mB-1)\tau\} + 1 \tag{9}$$

The dependence of the temperature θ upon time τ is shown in Fig.7.

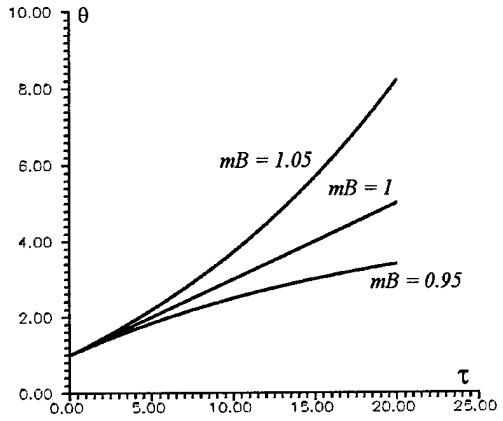

Fig.7. Bifurcation of linerized solution of energy equation at the initial point.

One can see that in the initial moment three cases are available that are controlled by the parameter mB-1. If mB>1 then the clot grows exponentially; if mB=1 then this growth is linear, and if mB<1 then the temperature quickly comes to the saturation. During the time all curves come to saturation (Fig.8) but its level is quite different.

One can note also that if clot form is a stretched cylinder the geometrical factor is to be taken into account

Considering such a cylinder as a number of elements regarded above it needs to take instead of (17):

$$B' = B \cdot l^2 / L^2$$

where l is the width of cylinder and L is its length.

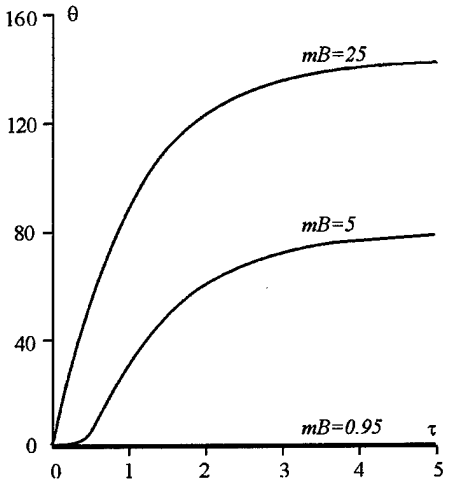

Fig.8. Dimensionless clot temperature 0 vs time τ.

3. Electrode Effects

In order to estimate an electrode wall effect on the energy balance due to resistive layer near «cold» wall, the resistance of the boundary layer R_{bl} is introduced in the expression for Joule heat release in the form:

$$q = \left(\frac{E}{R_0 + R_{bl}} \right)^2 R_0 \frac{1}{V_m} \qquad (10)$$

Than the energy equation (7) is transformed to the form

$$\frac{\partial\theta}{\partial\tau}=\frac{B\exp\{m(1-1/\theta)-\tau\}}{\left(1+\frac{R_{bl}\sigma_0 V_m}{S_0}\exp\{m(1-1/\theta)-\tau\}\right)^2}-\lambda_T\frac{\theta}{l_D^2\rho C_p\Omega}f_D$$

The dependence of the temperature q upon time t calculated with this equation is shown in Fig.9.

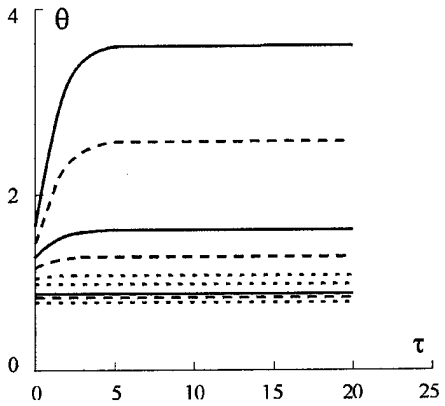

Fig.9.

A linearized expression similar to (9) is now as following

$$\theta(\tau)=\frac{B}{\omega(1+\xi)}\frac{\exp\{\omega\tau\}-1\}}{(1+\xi\exp\{\omega\tau\})}+1 \qquad (11)$$

where

$$\omega=\frac{mB}{(\xi+1)^2}-1\ ,\ \xi=\frac{R_{bl}\sigma_0 V_m}{S_0}.$$

Saturation with level θ_{lim}, depended upon ξ, can be seen in Fig.10.

$$\theta_{\lim}(\xi) = 1 + \frac{B}{|\omega(\xi)|} \cdot \frac{1}{1+\xi} \cdot \begin{cases} \frac{1}{\xi}, \omega(\xi) > 0 \\ 1, \omega(\xi) < 0 \end{cases},$$

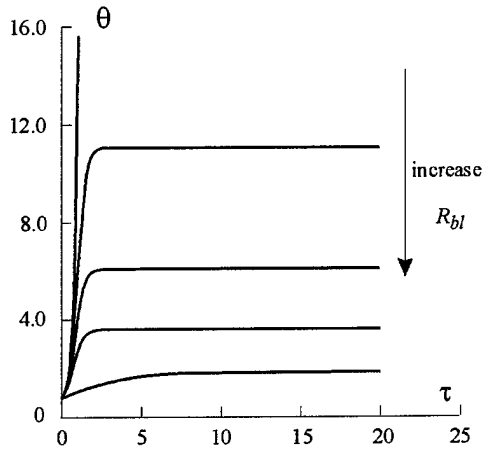

Fig.10.

i.e. quickly decrease with increasing ξ. Thus taking into account the wall effect results in limitation of exponential growth of the temperature.

4. MHD Generation of Turbulence.

The model described above regards the effect of turbulence coming into flow from outside, but if there is some external force turbulence is born in process of movement directly by non-potential part of one. Further evaluations permit to define characteristic scale of turbulence, fluctuation velocity and accordingly coefficient of turbulent diffusion. We assume for simplify that fluid is incompressible.

Equation for vorticity

$$\frac{\partial(\mathrm{rot}\,\mathbf{v})}{\partial t} = \mathrm{rot}[\mathbf{v}\times\mathrm{rot}\,\mathbf{v}] + \frac{\mathrm{rot}\,\mathbf{f}}{\rho} \qquad (12)$$

where **f** is external volume force, and v is fluctuation of velocity.

Multiplying by rot v on the left (in this case first term on the right is equal zero) integrate in the volume for getting of average value

$$\left\langle(\mathrm{rot}\,\mathbf{v})^2\right\rangle \equiv \frac{1}{V}\int(\mathrm{rot}\,\mathbf{v})^2\,dV$$

$$\int_V \frac{1}{2}\left(\frac{\partial(\mathrm{rot}\,\mathbf{v})^2}{\partial t}\right)dV = \int_V \frac{\mathrm{rot}\,\mathbf{v}\;\mathrm{rot}\,\mathbf{f}}{\rho}\,dV =$$

$$= \int_V \frac{\mathrm{rot}\,\mathbf{v}\;\mathrm{rotrot}\,\mathbf{f}}{\rho}\,dV + \int_S \frac{[\mathbf{v}\times\mathrm{rot}\,\mathbf{f}]_n}{\rho}\,dS$$

Hear the formula of vector analysis $\mathrm{div}[\mathbf{a}\times\mathbf{b}] = (\mathbf{b}\,\mathrm{rot}\,\mathbf{a}) - (\mathbf{a}\,\mathrm{rot}\,\mathbf{b})$ and Gauss theorem has been used.

Assume, that **f** is stepwise function, that is:

$$\mathbf{f} = \begin{cases} \mathbf{f}, \text{ insideof theclot} \\ \mathbf{0}, \text{ elsewhere} \end{cases}$$

we get that first term on the right is equal zero.

In this way by order value:

$$\frac{\partial < (\mathrm{rot}\,\mathbf{v})^2 >}{\partial t} \approx \frac{Sv}{\rho V}\frac{\delta f}{l} \qquad (13)$$

where S, r are characteristic bound surface and density, l is characteristic length of force jump, $\delta\mathbf{f}$ ($\equiv$ $\mathbf{f}$ in our case) is jump itself and $\mathbf{v}$ is characteristic fluctuation velocity.

Equation for velocity we can present in such form:

$$\frac{\partial(\mathbf{v_0}+\mathbf{v})}{\partial t} = -\nabla\left(\frac{p_0}{\rho}+\frac{\mathbf{v_0}^2}{2}\right) - \left(\frac{p}{\rho}+\frac{\mathbf{v}^2}{2}\right) -$$

$$-\nabla(\mathbf{v_0}v) + \frac{\mathbf{f}}{\rho} \qquad (14)$$

where $\mathbf{v_0}$, p_0 are velocity and pressure of fluid movement v is fluctuation of velocity and p is fluctuation of pressure.

Multiplying by $\mathbf{v}$ on the left, canceling cross products between basic quantities and fluctuation quantities we integrate for getting $<\mathbf{v}_2>$:

$$\frac{1}{2}\frac{1}{V}\frac{\partial < \mathbf{v}^2 >}{\partial t} = -\int_V \mathbf{v}\nabla\left(\frac{p}{\rho}+\frac{\mathbf{v}^2}{2}\right)dV -$$

$$-\int_V \mathbf{v}\nabla(\mathbf{v}_0\mathbf{v})dV + \int_V \frac{\mathbf{vf}}{\rho}dV$$

First two terms on the right are common gas dynamics terms, but we have interest only in the last one, which is concerned with volume force and hence we remain only this term.

Thus:

$$\frac{\partial < \mathbf{v}^2 >}{\partial t} \approx \frac{fv}{\rho} \qquad (15)$$

Now evaluate turbulent movement scale.

For this purpose, divide square of vorticity by square of velocity, regarded that characteristic times of value change are the same.

$$\lambda^2 = \frac{fv}{\rho}\frac{Svf}{lV\rho} = \frac{lV}{S} \qquad (16)$$

Average fluctuation velocity we get from (15), left side of which is turbulent energy dissipation.

In this manner: $fv/r=\varepsilon=v^3/l$, therefore

$$v = \sqrt{\frac{f\lambda}{\rho}} = \left\{\frac{lV}{S}\frac{f^2}{\rho^2}\right\}^{1/4} \qquad (17)$$

For diffusion coefficient:

$$D = \lambda v = \left\{\frac{l^3V^3}{S^3}\frac{f^2}{\rho^2}\right\}^{1/4} \qquad (18)$$

Returning to integrate volume and integrate surface can be gotten: $L^2 l \le V \le L^3$ (L is characteristic size of the clot) $S \sim L^2$, thus:

$$l^2 \le \lambda^2 \le lL$$

$$\left(\frac{lf}{\rho}\right)^{1/2} \le v \le \left(Ll\frac{f^2}{\rho^2}\right)^{1/4} \qquad (19)$$

$$\left(\frac{l^3 f}{\rho}\right)^{1/2} \le D \le \left(\frac{L^5 l^5 f^2}{\rho^2}\right)^{1/4}$$

Note also, that in above formulas dependents on the time is implicit, resulted from $l \approx \sqrt{Dt}$.

5. Energy Effects of Turbulence in Presence of Magnetic Field.

Let's consider again the problem solved in Section 2 in presence of magnetic field **B** perpendicular to electrodes.

Again shall search the decision for the region occupied by the clot fraction being not affected by diffusion.

Then energy equation is:

$$\rho c_p \frac{\partial T}{\partial t} jE_0 \qquad (20)$$

where E_0 — external electric field and j — volume average current density.

From section 2 follows, that it is possible to define j as:

$$j = \sigma_0(T)(E_0 - uB)e^{\Omega t} \qquad (21)$$

where u — average flow velocity.

In this work Ω represents surface growth due to external turbulence as well as induced turbulence which is born by nonpotential force **j×B**.

In above section average fluctuation velocity scale v and turbulent movement scale l were estimated. In addition integral character of this and by virtue of integrated character of these parameters we can canceled from ideal-step distribution of force amplitude. Having entered an assumption, that the dependence Ωt — characteristic of induced turbulence on v and l like dependence for external can be received:

$$\Omega_f = \frac{f}{\rho u},$$

where f — non-potential force.

By virtue of independence of these two processes of surface change it is possible to present Ω as a sum:

$$\Omega = \Omega_0 + \Omega_f,$$

where Ω_0 — characteristic of external turbulence.

For simplicity now let's assume, that u=0 and unites (1) and (2) in a system, previously having reduced them to dimensionless variable:

$$\begin{cases} J = e^{m(1-1/\theta)} e^{(1+\alpha J)\tau} & (22) \\ \dfrac{\partial\theta}{\partial\tau} = \beta J & (22^*) \end{cases}$$

Here:

$$J = \frac{j}{\sigma_0 E_0};\ \ m = \frac{I_j}{2T_0};\ \ \theta = \frac{T}{T_0};\ \ \tau = \Omega_0 t$$

$$\alpha = \frac{\sigma_0 E_0 B}{\rho u \Omega_0} = \frac{\sigma_0 E_0 B}{\rho v_t^2 / \lambda_t};$$

$$\beta = \frac{\sigma_0 E_0^2}{\rho c_p T_0};\ \ J|_{t=0} = 1;\ \ \theta|_{t=0} = 1\ .$$

Expressing q from (22*) through J and substituting in (22) we shall receive:

$$\frac{\partial J}{\partial\tau} = \frac{\beta/m (m - \ln J - (1+\alpha J)\tau)^2}{1/J + \alpha\tau} \qquad (23)$$

$$J|_{\tau=0} = 1$$

The dependence of the current density J upon time t at B=(0;0,001;0,01;0,1;1;2) is shown in Fig.11.

As we see availability of a magnetic field strongly influences a maximum current in the clot.

Let's consider now the solution of (22), (22*) at $\tau \to 0$. Then:

$$\theta|_{\tau=0} = 1 + \left(\frac{\partial\theta}{\partial\tau}\right)_{\tau=0} \tau + K \approx 1 + \beta\tau$$

$$1 - \frac{1}{\theta}\bigg|_{\tau\to 0} \approx \beta\tau$$

$$\begin{cases} J = e^{(m\beta-1)\tau} e^{-\alpha\tau} \\ \dfrac{\partial\theta}{\partial\tau} = \beta\tau \end{cases}$$

at

$$\tau \ll \frac{1}{\alpha J}$$

$$J = e^{(m\beta-1)\tau}(1-\alpha J\tau)$$

$$J = \frac{e^{(m\beta-1)\tau}}{1+\alpha\tau e^{(m\beta-1)\tau}}$$

$$\frac{\partial\theta}{\partial\tau} = \frac{\beta e^{(m\beta-1)\tau}}{1+\alpha\tau e^{(m\beta-1)\tau}}$$

Then:

If 1) $mb=1$

$$\theta - 1 = \frac{\beta}{\alpha}\ln(1+\alpha\tau)$$

2) $mb \neq 1$

$\frac{\partial\theta}{\partial\tau} > 0$ always, let's consider second derivative

$$\frac{\partial^2\theta}{\partial\tau^2} = \frac{\beta e^{(m\beta-1)\tau}}{\left(1+\alpha\tau e^{(m\beta-1)\tau}\right)^2}(m\beta-1-\alpha\tau)$$

The sign of expression in brackets determines behavior of dependence.

At $m\beta-1>\alpha$ dependence represents saturation.

At $m\beta-1<\alpha$ there is an inflection point at $\tau_{per} = \frac{1}{m\beta-1}\ln\frac{m\beta-1}{\alpha}$.

It is seen that the inflection point for q is simultaneously point of a maximum for J.

That is:

$$J_{\max} = \frac{m\beta - 1/\alpha}{1 + \ln(m\beta - 1/\alpha)}, \text{ at } m\beta - 1 > \alpha$$

and

$J_{\max} = 1$ (at t=0) for $m\beta - 1 < \alpha$.

Thus, I\it could be concluded that in this Section a simplified model of clot deformation in turbulent flow has been developed. Energy balance inside the clot is controlled by two competing processes: (1) stretching of current lines due to exponential growth of clot surface, and (2) exponential growth of conductivity. Three types of clot temperature growth — exponential, linear, saturating are found. Criteria for these evolution mode has been obtained. Limiting growth wall effect was shown. The main turbulence parameters produced by magnetic field has been appritiated. Strong influence of magnetic field to maximum clot current was shown. Results of proposed model are in quantitative agreement with experimental observations.

Current Zero at Gaseous Circuit Breakers. Influence of Turbulence [13].

It can be easily seen that the behavior of the electric arc, particularly its extinguishing near the zero electric current point at the alternative voltage, is determined of course by the kinetic processes in the arc column. On the other hand, the background of these processes and according initial conditions are to a considerable extent dominated by the distributions of macroscopic parameters. These distributions must be calculated within the frames of hydrodynamic description so that the latter is a very important part of the problem under consideration. Because the gas motion in the considering situation is turbulent the velocity of the background motion is a random function of space and time variables. Unfortunately the intervals of time typical for electrodynamic and kinetic processes are too short for using any averaging procedure, so the standard models of fully developed turbulence [19] are not applicable in our case (neither in Euler nor in Lagrange language [15]). The alternative way in which some «incomplete» turbulence can be taken into account was proposed in [9]: this way is based on the fact that the material lines and surfaces at the presence of the random velocity field grow exponentially (see also [15]). Corresponding model of

the exchange of energy leads to the equation which solution shows some critical behavior. In this connection two final states appear to be possible — extinguishing of some plasma formation (the so called clot) or its developing [10]. The latter shows that such a model of «incomplete» turbulent phenomena could be suitable for our case, of course after generalization of the model with regard to the nonhomogeneous situation.

In addition to the affirmations mentioned above there is one more important reason for which one is to avoid the usual procedures of the statistical or time averaging (here and below we denote averaging by the brackets < >). Namely, it should be taken into account that electric conductivity is a very «strong» (see later) function of the temperature. Consequently one can write (at the nonuniform temperature distribution) neither

$$\langle\sigma\rangle = \langle\sigma(T)\rangle$$

nor $\langle\sigma\rangle = \langle\sigma(\langle T\rangle)\rangle$,

so that some different approach for the finding of the effective values of the conductivity (or resistance) must be found. Because the conductivity and, consequently, the electric arc is sharply non-uniform the main problem is to describe the behavior of such strongly non-uniform plasma influenced by the external (non-stationary) voltage. This problem is considered as follows.

According to [9] all the influence of the turbulent motion on the arc region comes to taking into account of the exponential growth of «material» lines and surfaces at given regions of the arc. Such a viewpoint on the random velocity field influence on the material lines and surfaces comes to work by G.K.Bathelor [14] (this work included an error which was remedied later in [20]. According to this viewpoint some average length of the material line, for instance, depends on time in the next form

$$L(t) = L(t_0)e^{\xi(t-t_0)}$$

where ξ is to be defined as a value of order of the «intrinsic» frequency of turbulent motion. In [9,10] slightly different quantity was used which depends on the whole range of turbulent frequencies so that it differs from ξ by some factor. In any case there is no way now to obtain some «exact» value of ξ in both approaches and as a final result it is to be estimated from the

experimental data. If turbulent motion is non-uniform in space and time according generalized relation takes the obvious form (we at once use it for infinitesimal element)

$$dx \Rightarrow dx \exp\left\{\int \Omega(x,t)dt\right\},$$

which will be used below.

Taking account of the fact that in our simulations we shall watch individual fluid particles it is easy to see that the intrinsic time variable t is to be given in the form

$$dt = \frac{dx}{u(x)}$$

where $u(x)$ is velocity distribution along the are column. This time variable is synchronized with the «external» time variable (time of the change of some external parameters, for instance, voltage $U(t)$) by some special simulation procedure.

Returning now to the main purpose of this work we are to write down the relations describing the mentioned above effects of turbulence on are behavior.

For the electric resistance of the arc element dx, for instance, it reads

$$dR = \frac{dx \exp\{\Omega(x),t\}}{\sigma(x)S(x)} \qquad (*)$$

where σ is the electric conductivity, S is the surface of the electric current «tube», Ω is the time scale factor reflecting the influence of turbulent motion; its dependence on distance x corresponds to possible non-uniformity of the arc region. Namely this quantity, $\Omega(x)$, is to be connected with turbulent characteristics. At this condition the Joule dissipation is

$$q(x,t) = \sigma(x)E^2(x)\exp\{-2\Omega(x)\cdot t\} \ ,$$

where $E(x)$ is (local) electric field. Using (*) one can write for the latter (j is electric current density)

$$E(x) = \frac{j}{\sigma} = \frac{U(t)\exp\{\Omega(x)\cdot t\}}{\sigma(x)S_0(x)\int_0^L dx \frac{\exp\{2\Omega(x)\cdot t\}}{\sigma(x)S_0(x)}}$$

where the symbol «0» corresponds to some initial conditions concerning current distribution, $U(t)$ is the arc voltage. The value σ depends explicitly only on the temperature, T, so that

$$\sigma = \sigma_0 \exp\left[\frac{I}{2kT}\left(\frac{1}{T_0}-\frac{1}{T}\right)\right] ,$$

where I is the ionization potential, k is the Bolzmann constant. With the energy equation in the form

$$\rho c_p \frac{dT}{dt} = q$$

and the equation for the electric circuit

$$\mathsf{E}(t) = \mathsf{L}\frac{dI}{dt} + IR$$

where L is the inductance, one can solve the problem of E, T and j definition, in the column of arc. Introducing some characteristic parameters p^* (pressure), I^*, R^*, assuming L to be the length of the arc and coming to dimensionless variables,

$$\tilde{q} = q/q^* = q\Big/\sigma_0\left(\frac{I^*R^*}{L}\right)^2 , \quad \tilde{p} = p/p^* , \quad R^* = \frac{L}{\sigma_0 S_0} , \quad I^* = U_0/R^* ,$$

$$\vartheta = T/T_0 , \quad \tilde{\sigma} = \sigma/\sigma_0 , \quad m = I/2kT_0 , \quad \tilde{E} = E\Big/\left(\frac{I^*R^*}{L}\right) ,$$

$$\tau = t/t^* \quad (t^* = \mathsf{L}/R^*) , \quad \tilde{i} = I/I^* , \quad \tilde{r} = R/R^* , \quad \tilde{\Omega} = \Omega \cdot t_q^* ,$$

$$\tilde{x} = x/L , \quad \tilde{U} = U/I^*R^* , \quad \tilde{S} = S_0\Big/L^2 , \quad \tilde{e} = \mathsf{E}/I^*R^* ,$$

one can write down the next equations

$$\tilde{\sigma} = \exp\left[m\left(1-\frac{1}{\vartheta}\right)\right] ,$$

$$\frac{d\ln\vartheta}{d\tau} = \frac{\gamma-1}{\gamma}\frac{t^*}{t_q^*}\frac{\tilde{q}}{\tilde{p}} , \qquad (**)$$

$$\tilde{q} = \tilde{\sigma}\tilde{E}^2 \exp\{-2\tilde{\Omega}\cdot\tau\} ,$$

$$\tilde{E} = \frac{\tilde{U}\exp\{\tilde{\Omega}\cdot\tau\}}{\tilde{S}_0\tilde{\sigma}\int_0^1 d\tilde{x}\,\frac{\exp\{2\tilde{\Omega}\cdot\tau\}}{\tilde{\sigma}\tilde{S}_0}} ,$$

$$\tilde{e}(\tau) = \frac{d\tilde{i}}{d\tau} + \tilde{i}\tilde{r} ,$$

where $t_q^* = p^*/q^*$, γ is specific heat ratio. We shall start with the solution of these equation in comparatively simple case when **L**=0. At this condition the equation (**) takes the form

$$\frac{d\ln\vartheta}{d\tau} = \frac{\gamma-1}{\gamma}\frac{\tilde{q}}{\tilde{p}} ,$$

$$\tilde{U}(\tau) = \tilde{i}\cdot\tilde{r} ,$$

where $\tau = t/t_q^*$ and $\tilde{U}(\tau)$ is some given function, for example, $U(t) = U_0 \sin\omega t$ where ωω is the frequency of the alternative voltage.

Because, on one hand the assumption on the exponential growth of the material lines in turbulent flow renders decisive influence on the arc behavior and, the other, both mentioned above theories of this effect are not too convincing one is to demonstrate it in some probable way.

Our demonstration is based on the representation of the random velocity field in a form of sum each term of which is an exact solution of 2-D Euler equation, for an incompressible fluid

$$\frac{\partial\mathbf{v}}{\partial t} + (\mathbf{v}\nabla)\mathbf{v} = -\frac{\nabla p}{\rho} ,$$

$$\mathrm{div}\,\mathbf{v} = 0$$

$$\mathbf{v} = \langle u, v\rangle$$

so that the stream function ψ_k is

$$\psi_k = A_k \cos(kx+\beta_k)\cos(ky+\gamma_k) ,$$

where A_k is amplitude, β_k and γ_k — some initial values of the phases. It is easy to verity that ψ_k satisfies stationary Euler equation in the form

$$\frac{\partial\psi}{\partial x}\frac{\partial\Delta\psi}{\partial y}-\frac{\partial\psi}{\partial y}\frac{\partial\Delta\psi}{\partial x}=0 \ .$$

Consequently we construct the kinematics of turbulence in the next form

$$u=-\frac{\partial\psi}{\partial y}=\sum_{k=1}^{n}kA_k\cos(kx+\beta_k)\sin(ky+\gamma_k) \ ,$$

$$v=-\frac{\partial\psi}{\partial x}=\sum_{k=1}^{n}kA_k\sin(kx+\beta_k)\cos(ky+\gamma_k) \ .$$

Placing some initial «spot» which boundary is a circle which diameter $D>2\pi/k_{\min}$ one can observe this spot developing which time and its boundary growth. The results are given in Fig.11. From the latter one can see that according length growth is really exponential. It is also seen that the form achieved shows its randomness except some regular «cross» (Fig.11) The nature of this «cross» can be clarified as follows. Let us consider the set of the point at which $u = v$ (for instance, we consider case $u,v>0$). At such condition the relation

$$\sin(kx+\beta_k)=\cos(kx+\beta_k)$$

and similar for y must be satisfied. Therefore

$$kx+\beta_k=2\pi n+\frac{\pi}{4} \ .$$

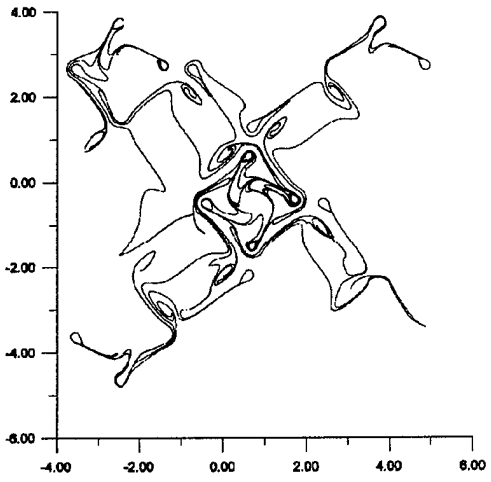

Fig11. The shapes of the original circular contour modified by a 'syntetic' turbulence field with different parameters.

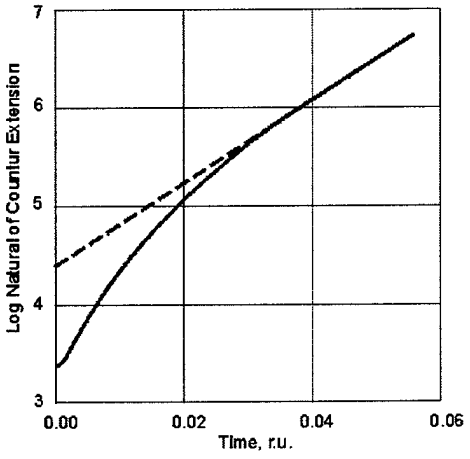

Fig.12. Confirmation of the logarithmic law of an arbitrary contour length growth.

It follows from the last relation that at $n=1$ and large k there are a lot of points with $u=v$ in the vicinity of the origin and namely these points give rise to such a «coherent» behavior of the boundary. Next we intend to eliminate such behavior by introducing some temporal factors into velocity definition and to connect the rate of the length growth to «turbulent» characteristics extracted from the values of according parameters.

It should be noted ones more that qualitative agreement between experimental observations (see Figs.2-4), others calculations (see Fig.5) and data obtained earlier in a gas-plasma flow (Figs.11) confirms the similarity of the processes in questions.

The most important practical conclusion is that so-called synthetic turbulence can be used in qualitative analysis of miscellaneous turbulence effect on physical-chemical processes defined by mixing stage.

IV. Reacting Volume Concept

The basic idea of reacting volume concept is already formulated in the previous Chapter. The equation of energy (6)

$$\rho C_p \frac{\partial T}{\partial t} = q - \lambda_T \nabla^2 T$$

includes the heat conductive member in the right hand side. The estimation of this expression used above is based on the assumption that a characteristic value of the temperature gradient ∇T is defined by a diffusion length l_D. The latter is estimated as $l_D \sim \sqrt{Dt}$ where D and t diffusion coefficient and time, correspondingly. Time t is calculated from the moment of the initial contact between the hot and cold fractions. Because of well known physical similarity between of the conductive heat transfer and species diffusion it is[possible to utilize the similar approach to treat the molecular mixing of fuel and oxidant, for example, by means of diffusion mechanism. The generalized driving force in this case is the species concentration gradient instead of the temperature gradient of the previous case. The liquid volume formed by contact surface between the two gaseous components (fuel and oxidant, for example) and by diffusion thickness l_D normal to this surface growths in time due to two factors at least. The first one is the increasing of diffusion length $l_D \sim \sqrt{Dt}$. In non-uniform non-steady state flows, especially in turbulent flows, the most important is the second factor – the (exponential) growth of the contact surface. The practical model of such a process has been developed in the study of a current carrying plasma clot evolution in turbulent flows and illustrated in the proceeding examples. Calling such an intermediate layer as *reacting volume one* can attribute to the fact that chemical reaction (burning as an example) between two reactants can occur typically if the local concentrations both reactants are high enough. Thus, reaction can start only inside of the diffusion layer. Furthermore, the maximal number of the reaction acts is proportional to the total number of reactants molecule in the diffusion layer. For more or less similar gases of fuel and oxidant the upper estimation of the acts is about one half of the total number of one of the reactant molecules in such a *reacting volume*.

It is clear that in the desirable case of effective burning in combustor chamber the reacting volume should include whole amount of reactants injected into the chamber. From the other hand the time of reacting volume formation is always finite and, for this reason, for effective combustion the residence time should be longer than the whole reacting volume formation.

It is obvious from the above simplified consideration that affecting both residence time and rate of reacting volume formation can result in combustion efficiency increasing.

The control of residence time is out of the scope of his study. Instead the methods of intensification of the reacting volume formation are a main goal of the study. Even more specific, the new 'advanced' technique of the mixing intensification will be checked – this is the MHD driven intensification.

The background of this technique is also presented in the previous Chapter when speaking about he MHD generation (modification) of turbulence. The physical background is the non-potential nature of the **j**×**B** body force that directly addresses to the turbulence (vorticity) production.

The additional profit of he MHD technique application can be the chemical effects due *to plasma chemistry mechanisms* which can take place because of rather high voltage discharge should be used .

In more detail the *electrodynamics* and *maghnetoihydrodynamics* components will be described in the next Report.

V. Concluding Remarks and Future Work

1. The methods of kinematics mixing described in the available technical papers and textbooks seems to be rather promising for the aims of this study.
2. The experience collected in the non-uniform gas-plasma flows study , especially connected to the plasma clots evolution in turbulent flows will be useful for the high speed combustion studies.
3. The estimation of the expected MHD mixing effects has shown that it will useful for the high speed combustion applications.
4. Preliminary analysis of the experimental validation potentiality resulted in positive conclusion.
5. The adaptation of existing numerical models for turbulent effects treatment in gas-plasma application to the combustion case is successfully started.

Part II

Contents

Introduction

This Report #2 is devoted to the adaptation of the existing CFD codes and chemical kinetics code to the case of interest I to study of advanced mixing in free high-speed jets. The preliminary plan was to limit this study only by mixing study. However during the preliminary analysis it was concluded that many important for future applications phenomena are expected under combined kinematics, dynamics and heat releases influence. MHD interaction which is assumed as a main newly proposed process for such an application involves (in any practical system based on thermal or weakly ionized gases) active particle such as ions, electrons, radicals, exited molecules an so on extremely important for the high temperature combustion especially in strongly non-uniform systems. Thus, the proper chemical kinetics scheme has to be included into the combined numerical simulation code. For these proposed we decided to use our experience and numerical codes used earlier to study the processes in miscellaneous plasma chemistry devices and in internal combustion engines. The KINEL chemical kinetics code was developed in IVTAN more then 10 years ago, checked in many practical applications. This code has been also modified to be used in the combined CFD code to describe multidimensional chemical reacting gases and plasmas.

Unfortunately, the full scale simulation of multi dimensional chemical reacting flow with extremely non-uniform MHD interaction is hardly possible in nearest future with the computers available. For these reasons the partial simulation is planned as a tool to understand the physical background of the method proposed. Thus, the next stage will be a simplified physical and corresponding numerical model development. The approach to such a development was already formulated in previous report # 1, where he concept of reacting volume was formulated. The reacting volume concept has to proved and if necessary modified with the data obtained with more sophisticated models.

In Section 1 the general physical formulation will be briefly discussed.
The section 2 is devoted to the systematic description of the CFD model to be used in multi-dimensional simulations.
The Section 3 presents an example of 2 dimensional time dependent simulation of the electrical discharge channel moving through gaseous media due to body force.
The section 4 presents a result of the hydrogen/air free stream combustion with a simplified 9-componenets species scheme.
In the last section future steps is briefly characterized.

1. Mixing at Contact Surface in Turbulent Co-Flow Streams

As an example of practical case the free stream jet combustion is considered. It assumed that two parallel jets – gaseous fuel and air of equal absolute velocity are created. The main point of interest is the contact surface between these two components. In the case of different velocities the Helmholz-Kelvin instability develops very fast. Such an instability process provides turbulization and corresponding turbulent mixing zone development. From he point of view of free stream combustion the formation of turbulent mixing zone is extremely positive feature. As we already discussed in the previous report #1 the turbulent mixing provides in fact increasing the effective square of the contact surface. Increased contact surface results in intensification of the total diffusion fluxes which are only responsible mechanism to prepare flammable fuel-oxidant mixture at molecular level.

The very qualitative vision of the turbulent mixing development at the contact surface is presented in Fig.1 as it can be observed in moving reference frame. The mutual penetration one gas component into the other one is characterized in time by multiplication of characteristics linear scale. It was shown in previous study that such a scale multiplication results in exponential growth of he contact surface in particular.

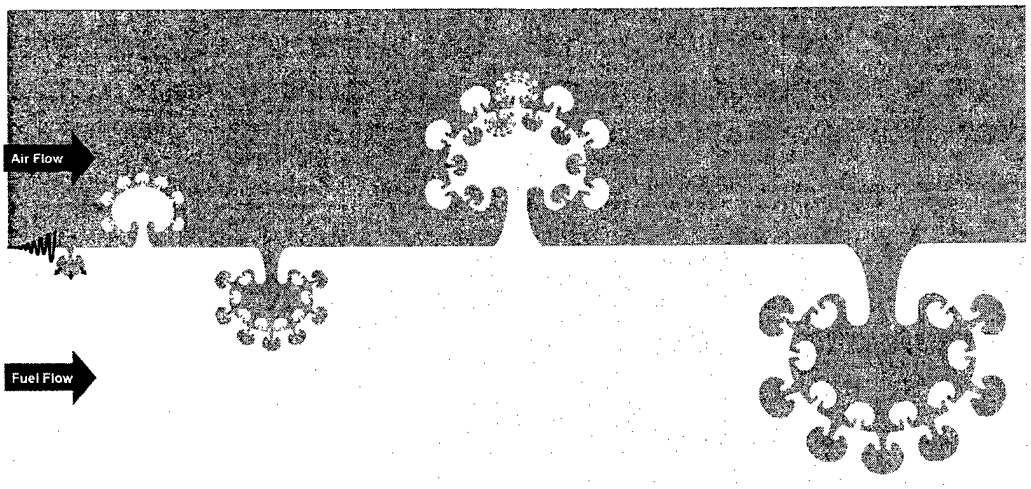

Fig.1. Schematic of 'turbulent mixing' at a contact surface between two co-flow streams

However despite of the exponential growth, which is defined by a characterization frequency of the particular turbulence for practical application, such a turbulence mixing can be

not enough fast. This is because of the residence time is very often very short for high-speed combustion chamber.

To intensify the contact surface growing the additional mechanism of mixing has been proposed. This mechanism involves high intensity body forces acting on the artificially created electrical current channels (arcs) if the external magnetic field of a proper orientation has been applied. As it will be demonstrated in the Section 3 such a current channel can be shifted across a flow from one component (fuel or air) to the neighboring jet (air or fuel, correspondingly). In small time scale this process is observed as "mushroom" developing across the contact surface. From the point of view of the multi scale turbulent approach MHD powered mixing results in modification (in the proper direction) of the integral characteristics of turbulence such as characteristic turbulence velocity (frequency, mixing length and so on).

As a very important additional advantage of the MHD forced mixing of fuel-oxygen system is automatically provided ignition and combustion stimulating factors: active particles (radicals) and electrical heating.

In order to check the real effect of such an 'advanced mixing' the second key process should be explicitly described – diffusion. In the case of a direct simulation of a single mushroom development it can be provided with the combined model described in the next section. However for multi discharge non-regular case we plan to use an simplified 'engineering' model based on several semi-empirical effective parameters.

2. Governing equations

Two-dimensional Navier-Stokes and species transport equations for a chemically reacting gas of N species in electric/magnetic field are given by

$$\frac{\partial \mathbf{U}}{\partial t}+\frac{\partial \mathbf{F}}{\partial x}+\frac{\partial \mathbf{G}}{\partial y}+\frac{\partial \mathbf{F}_v}{\partial x}+\frac{\partial \mathbf{G}_v}{\partial y}=\mathbf{S} \quad , \tag{1}$$

where

$$\mathbf{U}=\left(\rho,\rho v_x,\rho v_y,\rho E,\rho Y_1,\mathrm{L}\ ,\rho Y_N\right)^T$$

$$\mathbf{F}=\left(\rho v_x,\rho v_x^2+P,\rho v_x v_y,v_x(\rho E+P),\rho v_x Y_1,\mathrm{L}\ ,\rho v_x Y_N\right)^T$$

$$\mathbf{G}=\left(\rho v_y,\rho v_x v_y,\rho v_y^2+P,v_y(\rho E+P),\rho v_y Y_1,\mathrm{L}\ ,\rho v_y Y_N\right)^T$$

$$\mathbf{F}_v=\left(0,\tau_{xx},\tau_{xy},Q_x,J_{x1},\mathrm{L}\ ,J_{xN}\right)^T$$

$$\mathbf{G}_v=\left(0,\tau_{xy},\tau_{yy},Q_y,J_{y1},\mathrm{L}\ ,J_{yN}\right)^T$$

$$\tau_{xx}=-2\mu\frac{\partial v_x}{\partial x}+\frac{2}{3}\mu\nabla v$$

$$\tau_{xy}=-\mu\left(\frac{\partial v_x}{\partial y}+\frac{\partial v_y}{\partial x}\right)$$

$$\tau_{yy}=-2\mu\frac{\partial v_y}{\partial y}+\frac{2}{3}\mu\nabla v$$

$$\nabla v=\frac{\partial v_x}{\partial x}+\frac{\partial v_y}{\partial y}$$

$$Q_x=-\lambda\frac{\partial T}{\partial x}+\sum_{i=1}^{N}h_i J_{xi}-\left(v_x\tau_{xx}+v_y\tau_{xy}\right)$$

$$Q_y=-\lambda\frac{\partial T}{\partial y}+\sum_{i=1}^{N}h_i J_{yi}-\left(v_x\tau_{xy}+v_y\tau_{yy}\right) \tag{2}$$

$$J_{xi}=-\rho D_{im}\frac{\partial Y_i}{\partial x}\quad ,\quad i=1,N$$

$$J_{yi} = -\rho D_{im} \frac{\partial Y_i}{\partial y} \quad , \quad i=1,N$$

In these equations, the physical variables are the density ρ, the velocity components v_x and v_y, the pressure P, the temperature T, the internal energy e, the total energy $E = e + \frac{1}{2}\left(v_x^2 + v_y^2\right)$. The mass-fractions of species and enthalpies are respectively Y_i and h_i. μ and λ are molecular viscosity and thermal conductivity, respectively, of the gas mixture. The diffusion fluxes, J_{xi} and J_{yi} are defined by Fick's law (2) and effective diffusion – coefficients of species are obtained as

$$D_{im} = \frac{1 - X_i}{\sum_{j \neq i}^{N} X_j / D_{ij}} \quad ,$$

where $X_i = Y_i \cdot W / W_i$ is the mole-fraction of i-th species, Wi is the molecular weight and $W = \sum_{i=1}^{N} Y_i / W_i$ is the mixture molecular weight. Binary-diffusivities, D_{ij}, molecular viscosity and thermal conductivity are evaluated using Chapman-Enskog theory and Wilke's mixing rule.

Species enthalpies, h_i, are expressed as follows

$$h_i(T) = h_{i,f} + \int_{T_{ref}}^{T} c_{pi}(T)\, dT$$

where $h_{i,f}$ as the formation enthalpy of species i, $c_{pi}(T)$ is the specific heat. Specific heat are approximated by 5-th order polynomials of temperature.

The mixture internal enthalpy and energy are defined as

$$h = \sum_{i=1}^{N} Y_i h_i(T) \quad , \quad e = h - P/\rho \quad .$$

The pressure is determined from equation of stage for ideal-gas mixture

$$P = \rho \overline{R} \cdot T \quad ,$$

where $\overline{R} = R^0/W$, R^0 is the universal gas constant.

Source-term accounts contributions from chemical reactions for species transport, forces from electro-magnetic interaction and the work of electro-magnetic field.

$$\mathbf{S} = \left(0, F_x, F_y, Q_E, \dot{w}_1, \cdots, \dot{w}_N\right)$$

Electro-magnetic sources

$$\mathbf{F} = \left(F_x, F_y\right) = \left[\mathbf{J} \times \mathbf{B}\right],$$

$$Q_E = \left(\mathbf{J} \cdot \mathbf{E}\right) - Q_{rad} \qquad (3a)$$

J is the electric current density and

B is the magnetic induction vector.

E is the electric field strength. Ohm's law is used to link **E** and **J**:

$$\mathbf{J} - \frac{\beta}{B}\left[\mathbf{J} \times \mathbf{B}\right] = \sigma\left(\mathbf{E} + \left[\mathbf{v} \times \mathbf{B}\right]\right) \qquad (3b)$$

β is so called Hall parameter and is generally approximated by function of pressure, temperature and magnetic field. Electrical conductivity, σ, can be approximated as function of temperature of kind: $\sigma(T) = A \cdot T^n \cdot e^{-\psi/T}$.

For the slow electro-magnetic field, (3b) can be enclosed by definition of electric scalar potential, **E**=-grad φ.

Q_{rad} in (3a) denotes the radiative losses approximated for optically thin media as

$$Q_{rad} = \varepsilon \cdot \sigma_{SB} \cdot T^4 \ ,$$

(4) where ε is the effective absorption coefficient and σ_{SB} is Stefan-Boltzman constant.

Chemical sources

The species rate of production, $\dot{w}_i$ are found as

$$\dot{w}_i = W_i \sum_{r=1}^{N_r} \left[\nu''_{i,r} - \nu'_{i,r}\right] \cdot \left(k_{fr} \prod_{l=1}^{N} c_l^{\nu'_{i,r}} - k_{br} \prod_{l=1}^{N} c_l^{\nu''_{i,r}} \right) \qquad (3c)$$

if any of N_r reactions can be written in the form

$$\sum_{l=1}^{N} \nu'_{l,r} X_l \quad \underset{k_{fb}}{\overset{k_{fr}}{\rightleftarrows}} \quad \sum_{l=1}^{N} \nu''_{l,r} X_l$$

In (3b) ν' and ν'' are the stoichiometric coefficients of forward and backward reactions, respectively.

$c_i = \rho \cdot Y_i / W_i$ are the mole concentrations,

$X_i = W \cdot c_i / \rho$ are the mole-fractions.

k_{fr} and k_{br} are forward and backward reactions rate constants, respectively.

Arrhenius form is assumed for k_{fr} and k_{br}:

$$k_{fr} = a \cdot T^b \cdot \exp(-Ea/T)$$

Solution method

System of equations (1) is discretized in time and space using finite-volume formulation:

$$\frac{\partial}{\partial t} \int_{\omega} \mathbf{U}\, d\omega + \int_{\partial\omega} (\boldsymbol{F} + \boldsymbol{F}_v)\, dS_\omega = \int_{\omega} \mathbf{S}\, d\omega \qquad (4)$$

for any computational cell of volume ω enclosed by the surface S_ω with outward unit normal $\mathbf{n}(n_x, n_y)$.

$$\boldsymbol{F} = (\mathbf{F} + \mathbf{F}_v)n_x + (\mathbf{G} + \mathbf{G}_v)n_y$$

If piece-wise constant or piece-wise linear distribution of variables is assumed within each control-volume (cell), the transient term may be represented as $\omega \cdot \frac{\Delta \mathbf{U}}{\Delta t}$, where Δt is time-step.

(4) can be written as follows

$$\frac{\Delta \mathbf{U}}{\Delta t} + \mathbf{R} = 0 \quad , \tag{4a}$$

where **R** is the residual-vector.

This system is integrated in time using explicit low-memory Runge-Kutta method:

$$\mathbf{U}_0 = \mathbf{U}^n$$

$$\mathbf{U}_i = U_o - \alpha_i \frac{\Delta t}{\omega} \mathbf{R}(\mathbf{U}_{i-1}) \quad , \quad I=1,N_i \tag{4b}$$

$$\mathbf{U}^{n+1} = \mathbf{U}_{N_i}$$

where $\mathbf{U}^n$ is the solution on time-level t^n and $\mathbf{U}^{n+1}$ is the solution on time-level

$$t^{n+1} = t^n + \Delta t$$

The time-step, Δt, is selected as minimum of convective and diffusive time-scales for all the mesh control-volumes. While source-terms for momentum and energy equations are computed explicitly, calculation of chemical species production rates is carried out implicitly employing special chemical-kinetics solver.

$$\langle \dot{w}_i \rangle = \frac{1}{\Delta t} \int_{t^n}^{t^{nn}} \dot{w}_i dt = \left(\frac{dw_i}{dt} \right)_{chem}$$

Integration in time is performed by the program KINEL developed in IVTAN Low-Temperature Plasma Division for solution of systems of ordinary differential equations of high stiffness inherent to problems with chemical and thermal non-equilibria. On every time-step, Δt, system (4c) is integrated based on "chemical" time-steps and implicit treatment of production-rates. The chemical time-steps are evaluated within KINEL on the base of eigen-values of chemical source-term Jacobian matrix. Low-cost LU-decomposition of Jacobian is applied on each chemical time-step to solve the system.

Implicit treatment of chemical source-term allows one to avoid strong restrictions to the gas-dynamic time-steps imposed by finite-rate chemistry.

The integration of inviscid and viscous flux-vector over the control-volume surface is performed as follows. One-integration-point on the each surface-element (cell-interface straddling two neighboring cells) is suitable to obtain both 1-st order solution (piece-wise constant variable distribution within the cell) and 2-nd order solution (piece-wise linear variable distribution) in space. The inviscid flux at the integration-point is found from exact solution of Riemann problem (Godunov' method), i.e.

$$\mathbf{F}_{ip} = \mathbf{F}(\mathbf{U}_{ip}), \text{ and } \mathbf{U}_{ip} = R_{ie}(\mathbf{U}_L, \mathbf{U}_R) \qquad (4d)$$

$R_{ie}(\mathbf{U}_L, \mathbf{U}_R)$ implys solution of Riemann problem between two states $\mathbf{U}_L$ and $\mathbf{U}_R$, left and right state-vectors on both sides of the inter-face. For two adjacent cells, P and E,

$$\mathbf{U}_L = \mathbf{U}_P + \psi_P(\nabla\mathbf{U}_P, \Delta\mathbf{r}_{PN})$$
$$\mathbf{U}_R = \mathbf{U}_E - \psi_E(\nabla\mathbf{U}_E, \Delta\mathbf{r}_{EN}) \qquad (4e)$$

$\nabla\mathbf{U}_{P,E}$ are the cell-centered gradients and Δr_{EM} is the vector directed from cell-center $P(E)$ to mid-point of the interface M. the gradient in each cell, $\nabla\mathbf{U}_P$, is calculated by the least-square method as minimum of functional

$$\Phi_P = \sum_{J\in\omega_P} \Delta_{JP}^2 \ ,$$
$$\Delta_{JP} = (\mathbf{U}_J - \mathbf{U}_P) - (\nabla\mathbf{U}_p \cdot \Delta\mathbf{r}_{Pj})$$

Here J stands for any cell from the stencil associated with cell P. usually, five-point stencil of the nearest neighbors (including P) is considered. The limiter-functions ψ_P's are evaluated to satisfy the monotonical distributions near the strong flow discontinuities. In the smooth-flow regions, the second-order accurate spatial distributions are recovered. In one-dimensional problem, this method becomes equivalent to the well-known Van Leer MUSCL method.

Viscous fluxes at cell interface may be constructed in two ways. In first may, the face-gradient is taken to be the algebraic average ot two cell-gradients described just above with adding up the projection of normal-derivative to prevent the non-physical oscillations. In second way, the gradient at interface is calculated by application of Gauss' theorem to auxiliary cell"

$$\omega_a(\nabla \mathbf{U}_M) = \int_{\partial\omega_a} (\mathbf{U}\cdot\mathbf{n}_a)\, dS_a .$$

Auxiliary cell represents the quadrilateral vortices of which are two cell-centers (P and E) and start-point and end-point of the interface segment itself. Both approaches were found to be equally appropriate.

System of gouverning equations is to be enclosed by the initial and boundary conditions. The following types of boundary conditions can be handled.

1) Inlet

The incoming flow compositions is specified and flow variables, ρ, $\mathbf{v}$,P are specified dependent Mach number value. For supersonic inflow all variables can be set. For subsonic inflow, total temperature, total enthalpy and flow angle are specified and iso-entropic relations are assumed to hold.

2) Outlet

On supersonic outlet all variables are extrapolated from the interior with 1st or 2nd spatial accuracy. Also, static pressure can be specified at the outlet boundary.

3) Solid Wall

Non-slip conditions are applied for viscous computations. Adiabatic or constant-temperature conditions are used for energy equation. Non-catalytic or prescribed-compositions conditions are used for species transport equations.

4) Symmetry

Normal-derivatives are set to zero for all the variables except normal velocity which is set to zero.

Depending on the problem, the elliptic problem for electric potential, which is the consequence of the system (3), can be solved. For this purpose, high-performance elliptic solver is employed based on Additive Correction Multigrid concept along with the Modified InComplete Choletski methoid.

3. Current Channel Propagation in External Magnetic Field

The evolution of the initially stated uniform arc in the magnetic field was computed as demonstration problem. The arc was assumed to be uniform in z-direction and magnetic field $\mathbf{B}=(0,B_y,0)$, B_y=1 Tesla, was specified in the domain 6×1.5mm in x- and y-directions, respectively. The uniform arc of 1mm diameter was positioned at the symmetry axis (y=0) and 1.5mm right of the left boundary. Initial temperature of the arc has been set to 9000K, which approximately corresponds to equilibrium between Joule dissipation and radiative cooling in the uniform arc.

Initial pressure of 1atm has been specified everywhere. The temperature of the ambient gas was set 300K. The total current 2A was assumed to flow through the arc.

From these considerations the two-dimensional problem on evolution of the arc can be solved. Two kinds of computations were carried out: inviscid (and thermally non-conductive) and viscous(thermally conductive). The flow fields at different time moments are shown in Fig.1 (inviscid) and Fig.2 (viscous). The temperature color-scale ranges from 300K to 22000K in all figures. Temperature contours are uniformly spaced with the difference 440K.

While the average velocity of the arc is nearly same for both calculations, the shape of it is quite different. Inviscid arc constricts in its leading part, whereas trailing part is strongly cooled. Viscous arc is more uniform during time period considered. However, the temperature drops below 4000K.

These calculations are considered as the preliminary stage of the whole problem.

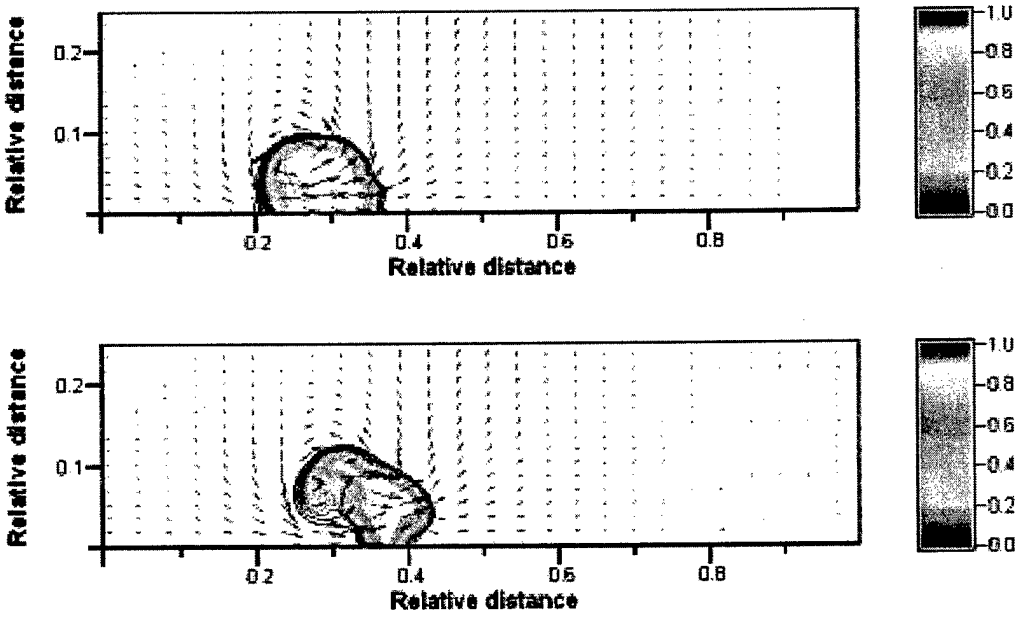

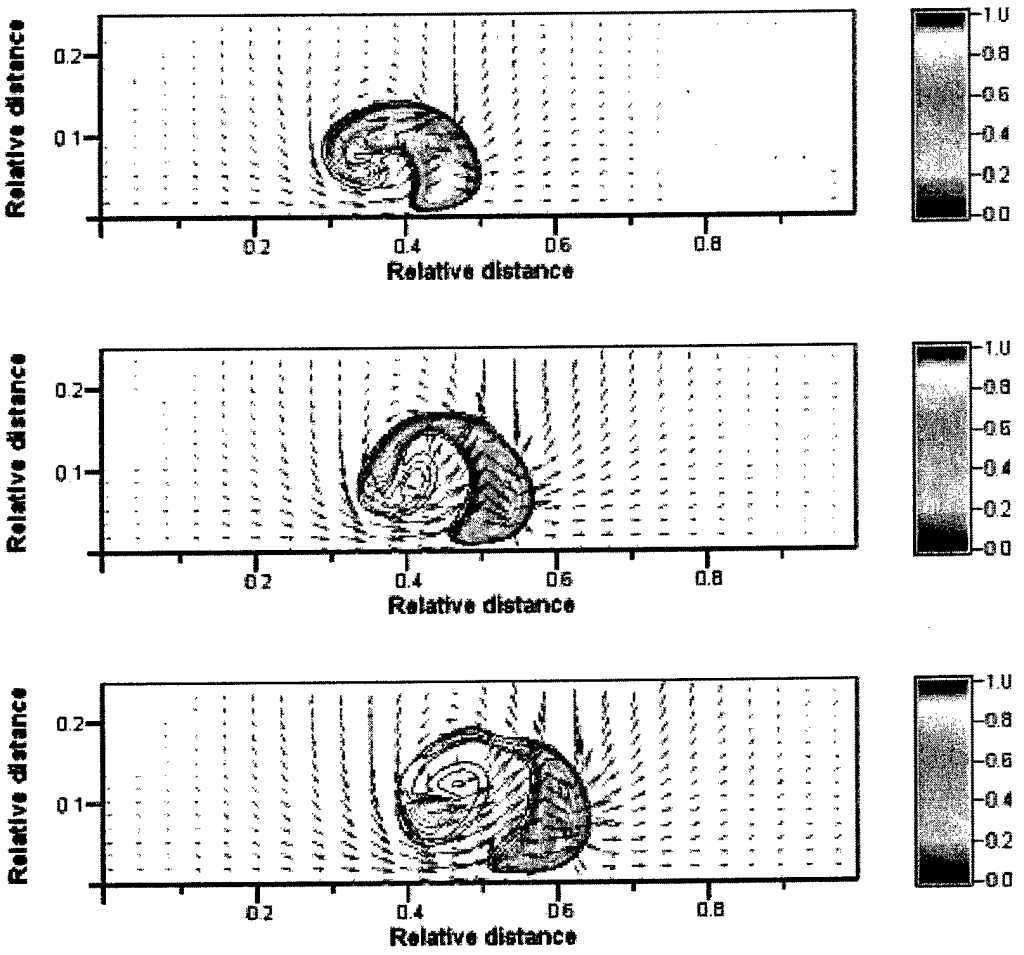

Fig.2. Temperature and velocity vectors at time-moments 10,20,30,40 and 50 mks (from up to down). Inviscid case. T_{max}=22000K, ΔT=440K.

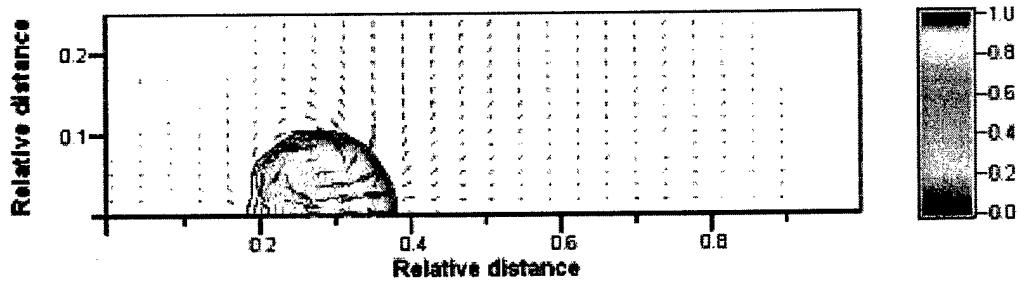

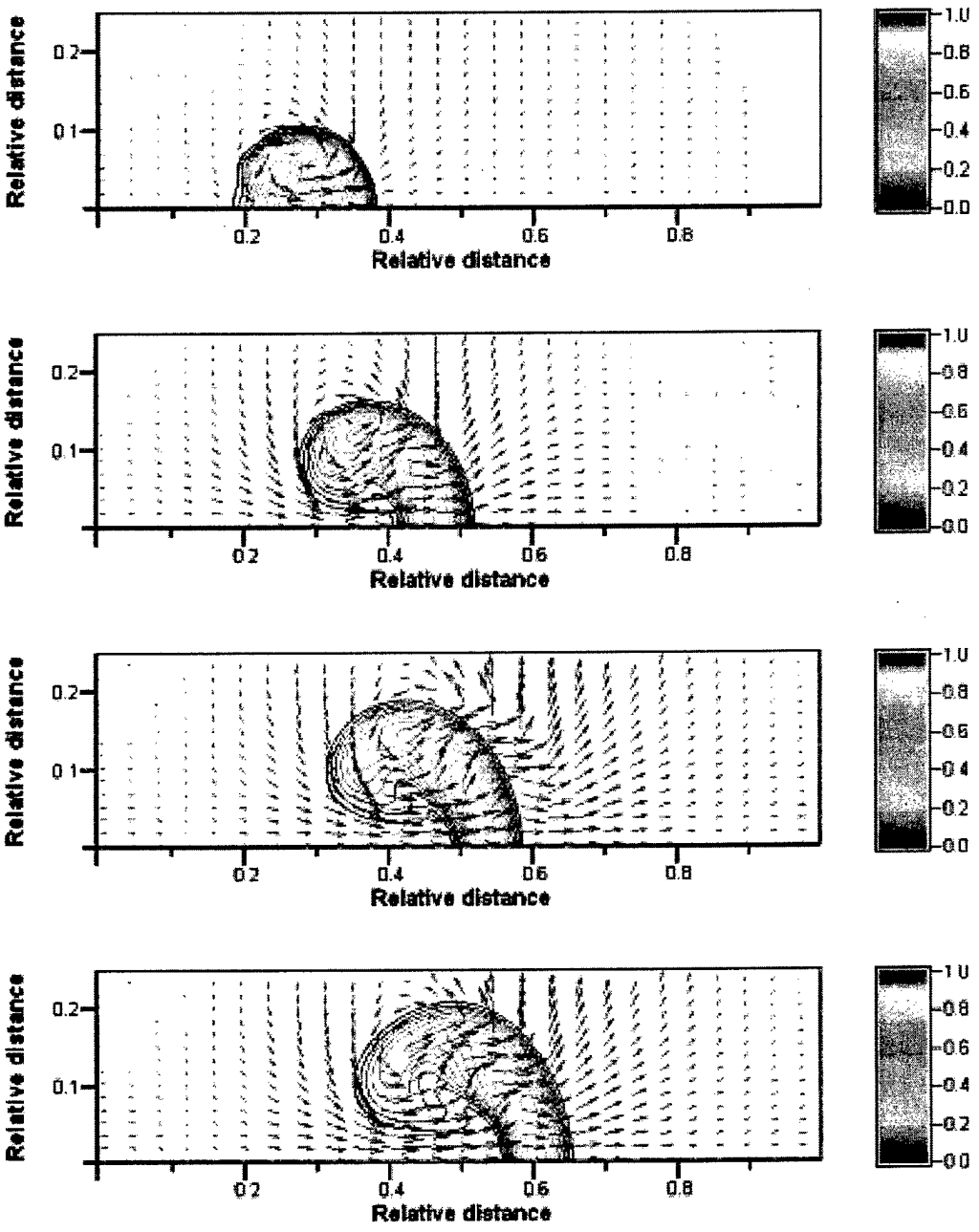

Fig.3. Temperature and velocity vectors at time-moments 10,20,30,40 and 50 mks (from up to down). Viscous case.

4. Reacting Volume Development in 1Dt Simulation

The general set of equations was reduced to 1Dt case to simulate a simplified case of reacting volume development in an axial symmetric configuration.

As a typical of scramjet composition the example of hydrogen/air system is considered.
The geometry assumed is two co-axial configurations consisting of internal hydrogen stream and external air stream. The radius of internal stream is 1 cm, and outer radius of external air stream is 2 cm.
It is assumed that any gas parameter is changing only in radial direction and in time.

Initial conditions are: uniform temperature $T = 1200$K, pressure $p = .1$ MPa and zero velocity.
The boundary conditions at the outer radius $r = 2$ cm are non-penetrated wall conditions.
Simplified widely used chemical kinetics scheme involving 42 reaction with 9 species is implemented:

1. H2+O2=OH+OH
2. OH+OH=H2+O2
3. OH+H2=H2O+H
4. H2O+H=OH+H2
5. H+O2=OH+O
6. OH+O=H+O2
7. O+H2=OH+H
8. OH+H=O+H2
9. O+H2O=OH+OH
10. OH+OH=O+H2O
11. H+H+M=H2+M
12. H2+M=H+H+M
13. H+O2+M=HO2+M
14. HO2+M=H+O2+M
15. OH+H+M=H2O+M
16. H2O+M=H+OH+M
17. HO2+H2=H2O2+H

18. H2O2+H=HO2+H2
19. HO2+HO2=H2O2+O2
20. H2O2+O2=HO2+HO2
21. H+HO2=OH+OH
22. OH+OH=H+HO2
23. H+HO2=H2O+O
24. H2O+O=H+HO2
25. H+HO2=H2+O2
26. H2+O2=H+HO2
27. O+HO2=OH+O2
28. OH+O2=O+HO2
29. OH+HO2=H2O+O2
30. H2O+O2=OH+HO2
31. OH+OH+M=H2O2+M
32. H2O2+M=OH+OH+M
33. HO2+H2=H2O+OH
34. OH+H2O=HO2+H2
35. HO2+H2O=H2O2+OH
36. H2O2+OH=HO2+H2O
37. H+H2O2=H2O+OH
38. H2O+OH=H+H2O2
39. OH+M=O+H+M
40. O+H+M=OH+M
41. O+O+M=O2+M
42. O2+M=O+O+M

Under conditions considered the diffusive combustion develops. The typical results are presented in following six plots.

In Fig.4 the radial temperature distributions developing in time are presented. It is clear from the plot that under considered conditions the combustion is diffusion control combustion self ignited by the initial rather high temperature. It is well known that such an air-hydrogen mixture is self-ignited when the temperature higher then 550-600C. The initial temperature assumed in this example provides high combustion rate. The maximal temperature about 3000 K is reached in .7 ms. It is

also seen that at the late stages of the process development the combustion rate decreases due to perhaps the increasing of diffusion length.

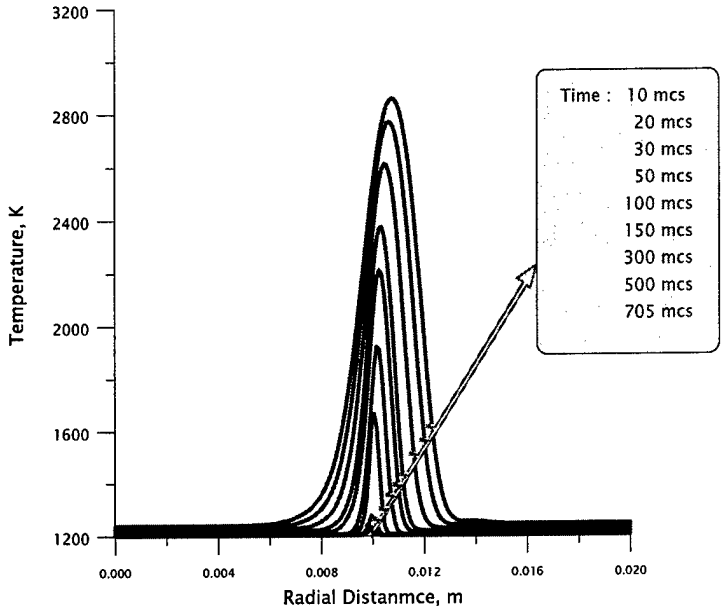

Fig.4 Development of Temperature Distribution across Reacting Volume

The heat release of combustion results in significant disturbances of pressure. At he initial stage of combustion compression waves are formed at the reacting volume. The Fig.5 illustrates the pressure distribution development in time. At the later stages the pressure changes more and more gradually corresponding to the process of the heat release in a closed vessel.

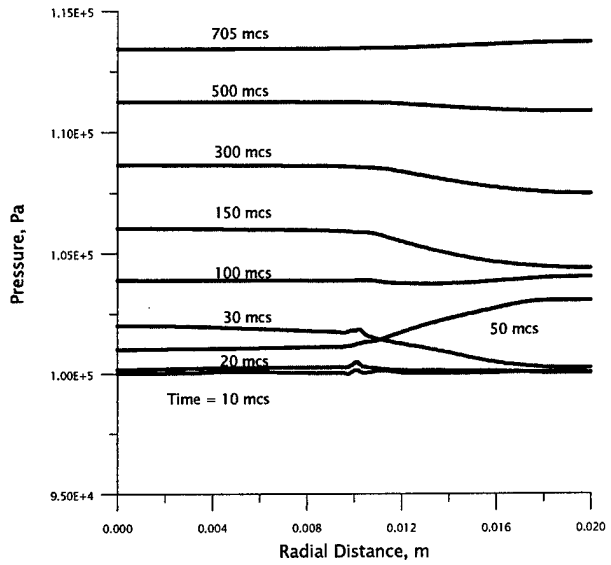

Fig.5 Development of Pressure Distribution across Reacting Volume

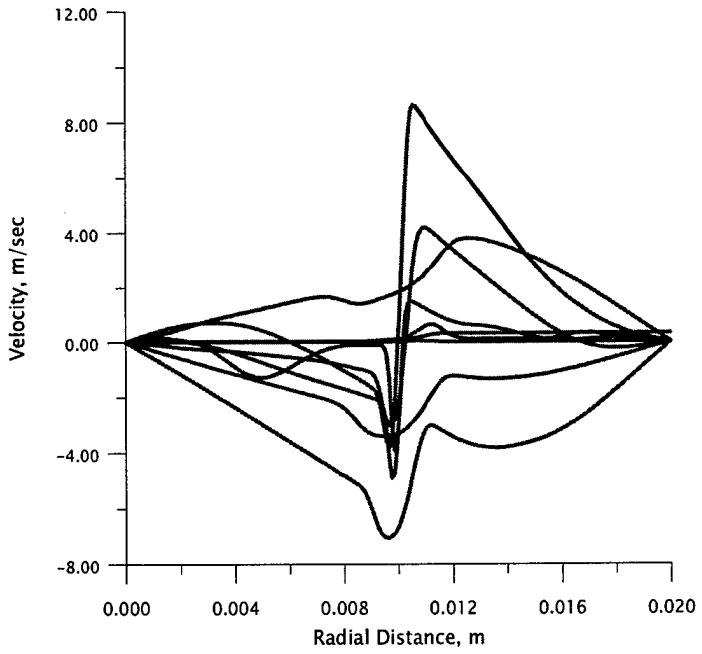

Fig.6 Development of Radial Velocity Distribution across Reacting Volume

The pressure disturbances result in radial velocity. Because of the boundary conditions related to the closed volume the velocity distribution is very non-uniform and non-regular in time

(see Fig.6). It should be noted that the amplitude of the radial velocity is very small and seems to be rather insignificant in future study of the combustion kinetics in free stream high-speed jets.

The formation of the reacting volume is illustrated in Fig.7 where the time variation of the radial distribution of two characteristics species are plotted. The first is the water weight fraction distribution, and the second – the nitrogen weight fraction distribution. The first value is a main product of the combustion process considered here. The second being fully non-changeable due to the chemical kinetics scheme used represents rather accurate the diffusion volume. It is seen that these two regions are very closed to each other confirming the fact that in this particular case the combustion is the diffusion-controlled combustion. A slight deformation of the nitrogen distribution at the outer border of the diffusion volume is caused by he the weak convection and characterizes the secondary effects which are very weak here.

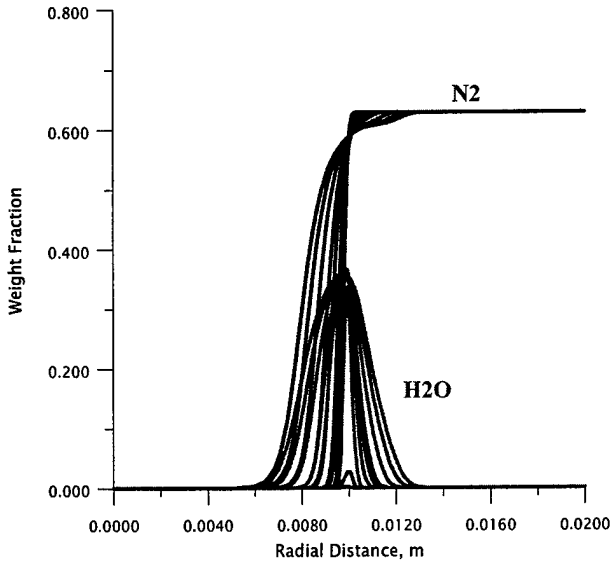

Fig.7. Development of Radial Distribution N2 and H2O across Reacting Volume

The full species information is presented in Fig.8. The radial distributions presented there correspond the time moment of 500 mcs when the combustion riches the full developed stage. Fom the analysis of the species distributions one can conclude that the process is non-monotonic in small scale consideration. For example the oxygen distribution reveals an intermediate minimum due to combined effect of diffusion and heating by heat release. At the same time we recognize that

such a non-notorious behavior is observed at very low level of oxygen concentration. Under condition different from the considered here this effects can be much more significant.

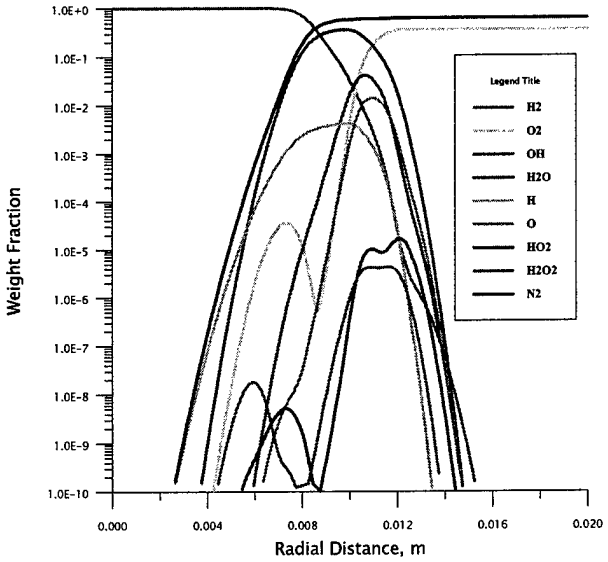

Fig.8 Main Species Distribution across Reacting Volume at the Time Moment of 500 mcs

The interesting fact is presented in the next Fig.9 where the water concentration and the temperature are presented for comparison. The non-trivial results here is that the peaks of the water concentration (combustion product) and the peak of the temperature resulting from heat release from the combustiom (water formation) are shifted of each other. The temperature 'propagates' in front of water formation. Again such an effect can be significant in future study of the more realistic case of combined effects of gas discharge drowned through the non-premixed fuel/air system.

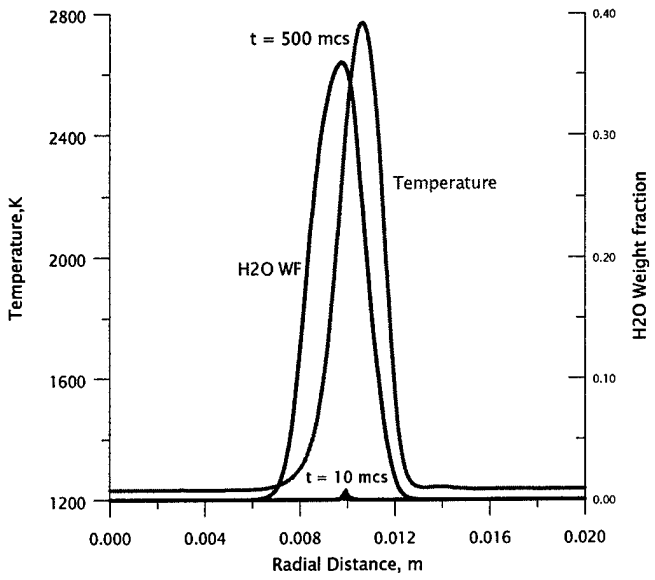

Fig.9. Comparison of Temperature and H_2O Weight Fraction Distributions across Reacting Volume at Two Time Moments 49 and 500 mcs.

Concluding this example presentation it could be recognized that the chemical kinetics simulation prepared for the future implementation into *combined advanced mixing simulation code* satisfies to desirable applications.

5.Concluding Remarks and Future Work

Two main component of numerical model of the advanced mixing powered by MHD body forces are developed.

The models are demonstrated with particular cases of MHD forced mixing and with combustion in diffusion mixing area.

The next step is a verification of combined model involving both key components.

Basing on the results of such of simulation a simplified integral model of the MHD forced mixing and combustion in reacting volume is being developed.

It was also found even on this preliminary stage that the MHD mixing has provided not only intensification of the mixing (passive combustion enhancement) but also the dramatically increased ignition effectiveness especially for practical important case of cool fuel jets.

Part III

1. MHD Driven Mixing at Contact Surface in Co-Flow Streams
2. Reacting Volume Development in 2D Simulation
3. Ignition and Combustion under MHD Stimulation
4. Experimental Validation Scheme
5. General Conclusion

1. MHD Driven Mixing at Contact Surface in Co-Flow Streams

As a typical configuration of the gas- fuel system in the combustion chamber of an air-breathing engine we will consider two co-flow streams. It is well known from classical fluid dynamics that the contact surface between two co-flow streams is absolutely unstable. The Kelvin-Helmholz instability destroys the contact surface resulting in multi scale chaotic flow, which can be considered as turbulent flow. It seems that the characteristic size of perturbed region growths downstream practically linear with the distance from the initial location (nozzle exit). Moreover one can assume that the rate of the perturbed region cross-section would be proportional to the difference of the tangential velocities of the streams.

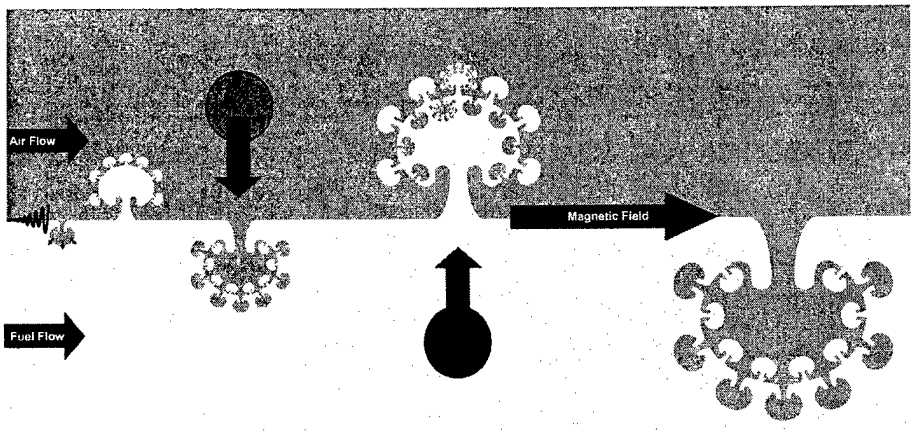

Fig.1. Schematic of MHD driven mixing at the contact surface in co-flow streams.

In a case of a single free jet we consider the interface surface created at two co-flow streams with the tangential velocities difference equal to the free jet velocity at the origin cross-section. For such a configuration the empirical law was formulated. This law says that characteristic cross-section size of the perturbed region growths downstream linearly with a rate factor as high as 0.25. We can adopt this law to estimate the cross-section characteristic size increasing *in time* rather than in space. Doing so we can find that the rate of the cross-section size growing is proportional to the co-

flow stream relative velocity. This rule results in an estimation of the perturbed region characteristic cross-section size at the contact surface of co-flow streams as a value proportional to the distance from the origin location with the factor .25 χ where χ is a reduced relative velocity

$$\chi = {}^{|v_1 - v_2|}\Big/_{(v_1 + v_2)}.$$

Thus, the maximal rate of the perturbed region growth corresponds to the free jet case, and minimal rate corresponds to the 'neutral' flow when the velocities of both streams are equal to each other. It should be noted that the perturbed region mentioned above is the 'turbulent' mixing region. Only in this region the *reacting volume* can develop.

In this study we are interested to assess the role of an external mechanism stimulating turbulence mixing. For this purpose it is convenient to consider at first a neutral case with no velocities difference. Thus, no turbulence mixing will occur. Instead only MHD driven mixing will take place. One of the simplest ways to provide the MHD driven mixing is:

a. To provide electrical discharge channel in some vicinity of the contact surface. This discharge channel with a current I would be directed along the contact surface and perpendicular to the flow velocity.
b. To provide external magnetic filed of the magnetic induction B co-oriented along the flow.
c. Thus, the body force $\mathbf{j}\times\mathbf{B}$ normal to the contact surface will drive the current channel across the flow. Choosing the proper current direction one can provide the penetration of the current channel from the one stream to another. Such a penetration results in extra mixing due to obvious growth of the area of the contact surface.

Moreover the current channel created and supported by an external electric field is an region with rather high energy release that results in the temperature increasing and, if the electric filed high enough, in production of active particles - *radicals* which is primary importance to initiate the chain combustion reaction.

Further in this report we will mine the first two results: mixing through the contact surface growth, and ignition of combustion due to heat release in the current channel.

2. Reacting Volume Development in 2D Simulation

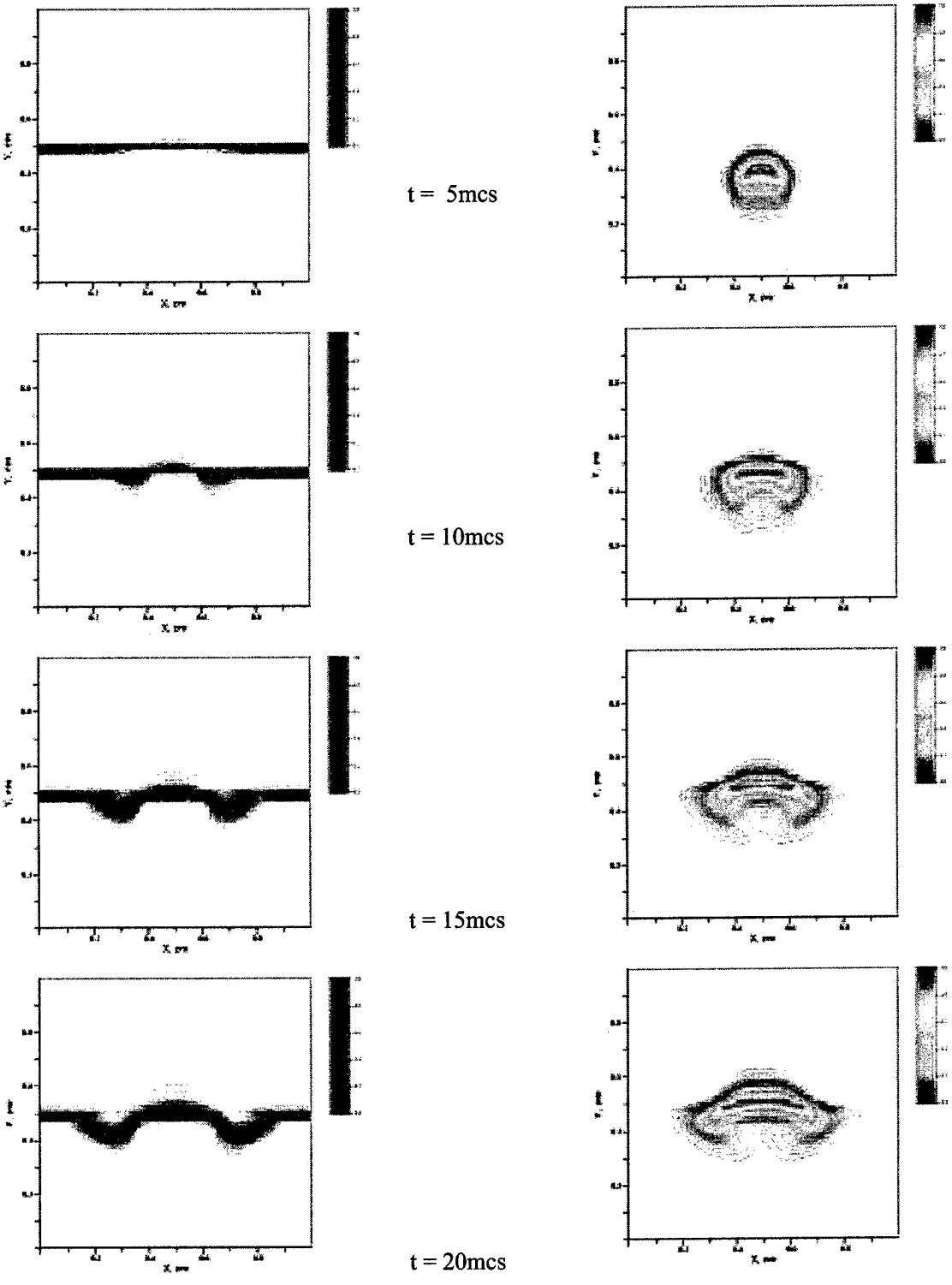

Fig.2. The mass fractions of hydrogen and water (left) and temperature(right) for Case 1 (no chemistry).

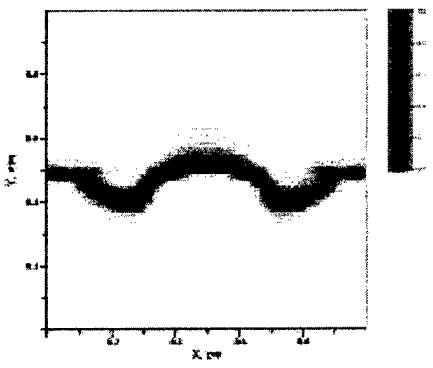

t = 25mcs

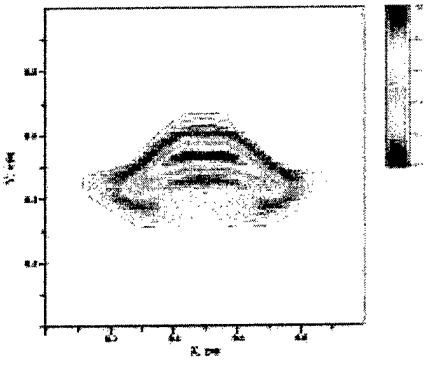

3.

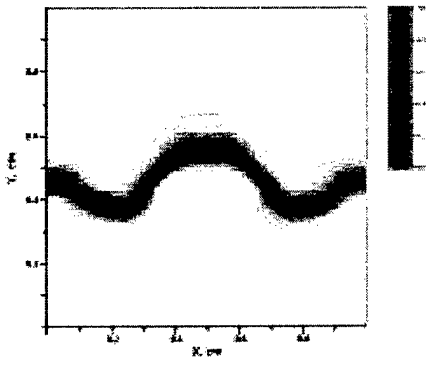

t = 35mcs

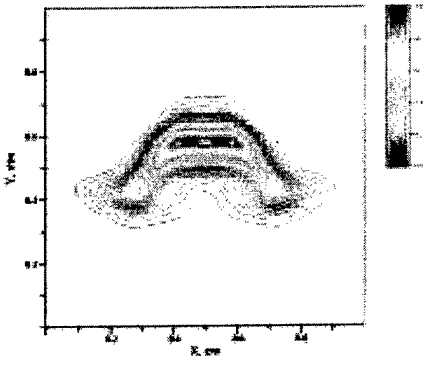

4.

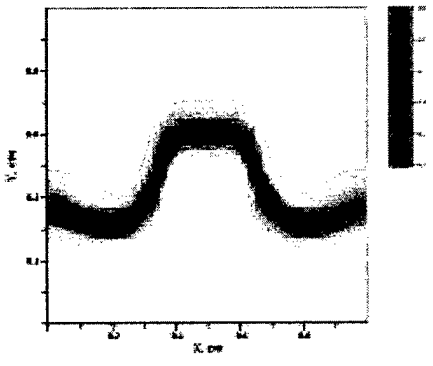

t = 50mcs

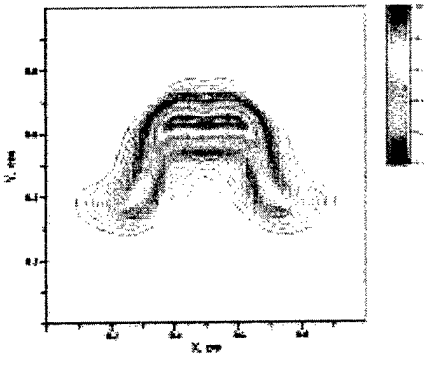

5.

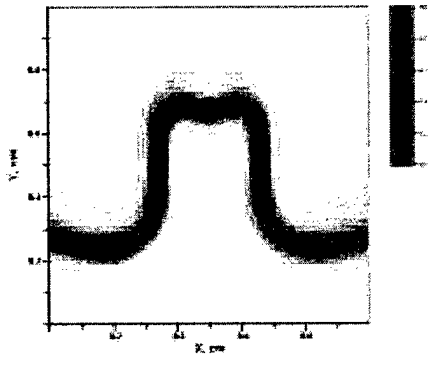

t = 70mcs

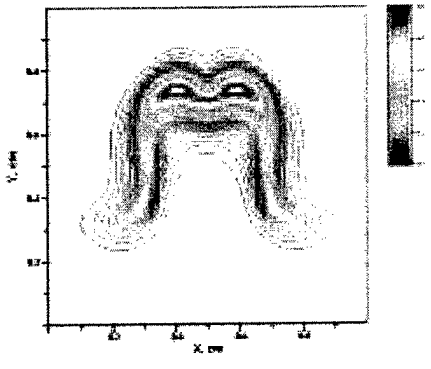

6.

Fig.2. The mass fractions of hydrogen and water(left) and temperature(right) for Case 1 (no chemistry, cont.).

In the Fig.2 of this section the *reacting volume* development in time is illustrated.
In configuration of the Fig.1 with no relative velocity the problem of the MHD driven mixing is considered. It is assume that total current of a single discharge channel as high as 10 Amps; the external magnetic field is 3 T. the gas properties are assumed to be correspondent to the air-hydrogen flow. In this particular case no chemical reaction is considered. At the same time all diffusion, heat conductance and viscosity effects are included as it has been defined in Part II numerical model. The initial static pressure is 1 atm. The initial gas temperature is 300K, the initial temperature inside the arc – discharge channel is assumed to be equal to 6000K that more or less characteristic temperature for the considered conditions. The arc channel diameter is 2 mm, the initial location of the discharge channel in 2 mm from the contact surface. In the figs hydrogen, and the upper occupy the lower part of the calculated domain by air.
The time period of the first 70 mcs has been considered. It can be easily seen from the pictures that the diffusion starts immediately creating a reacting volume. The rough estimation of such a process made in Part I of this report is qualitatively confirmed. In time the convection influence becomes more and more significant. The square of the interface surface increases especially when the discharge current has penetrated the interface. In case of discharge initiation in the hydrogen (very light gas) the discharge channel deforms significantly while approaching the heavy gas border spreading along the interface.
Probably due to rather low velocity of the discharge channel the diffusion region at the tip of the cross-section of the current duct differs not significantly from those at the peripheral region of the domain. It means that the reacting volume can be estimated as a product of the interface surface square S_c and diffusion thickness $\delta_D \approx \sqrt{Dt}$. More accurate conclusion at this stage of study is problematic because of many mechanisms affecting the formation of the *reacting volume* are involved. For example, the temperature dependence of the diffusion, real gas properties, and others factor are obviously important.
As it was expected the nature of the MHD enhancement of the *kinematics mixing* is the vorticity of the Lorentz body force. The flowfield presented in the previous Part II is clearly intensively vortex. The vorticity (simplified turbulence) results in fast increasing of any fluid surface located in such a flow.

The heat release effect in an applied electric field is illustrated by the second column in Fig.2 where the temperature filed evolution is presented. It can be observed that the area of the hot gas increases as well.

In the next section we will examine the reaction effects on the mixing and combustion under conditions considered.

3. Ignition and Combustion under MHD Stimulation

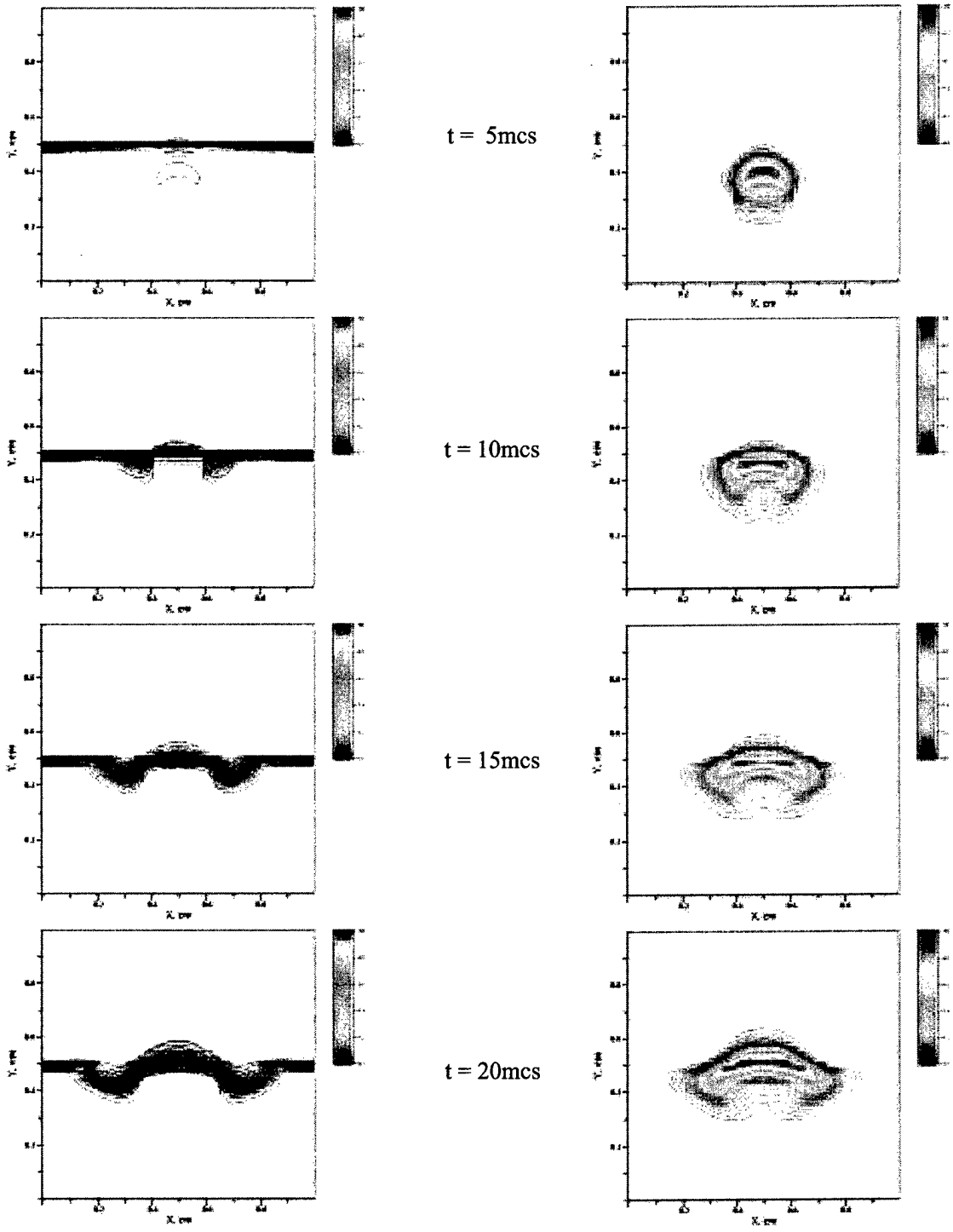

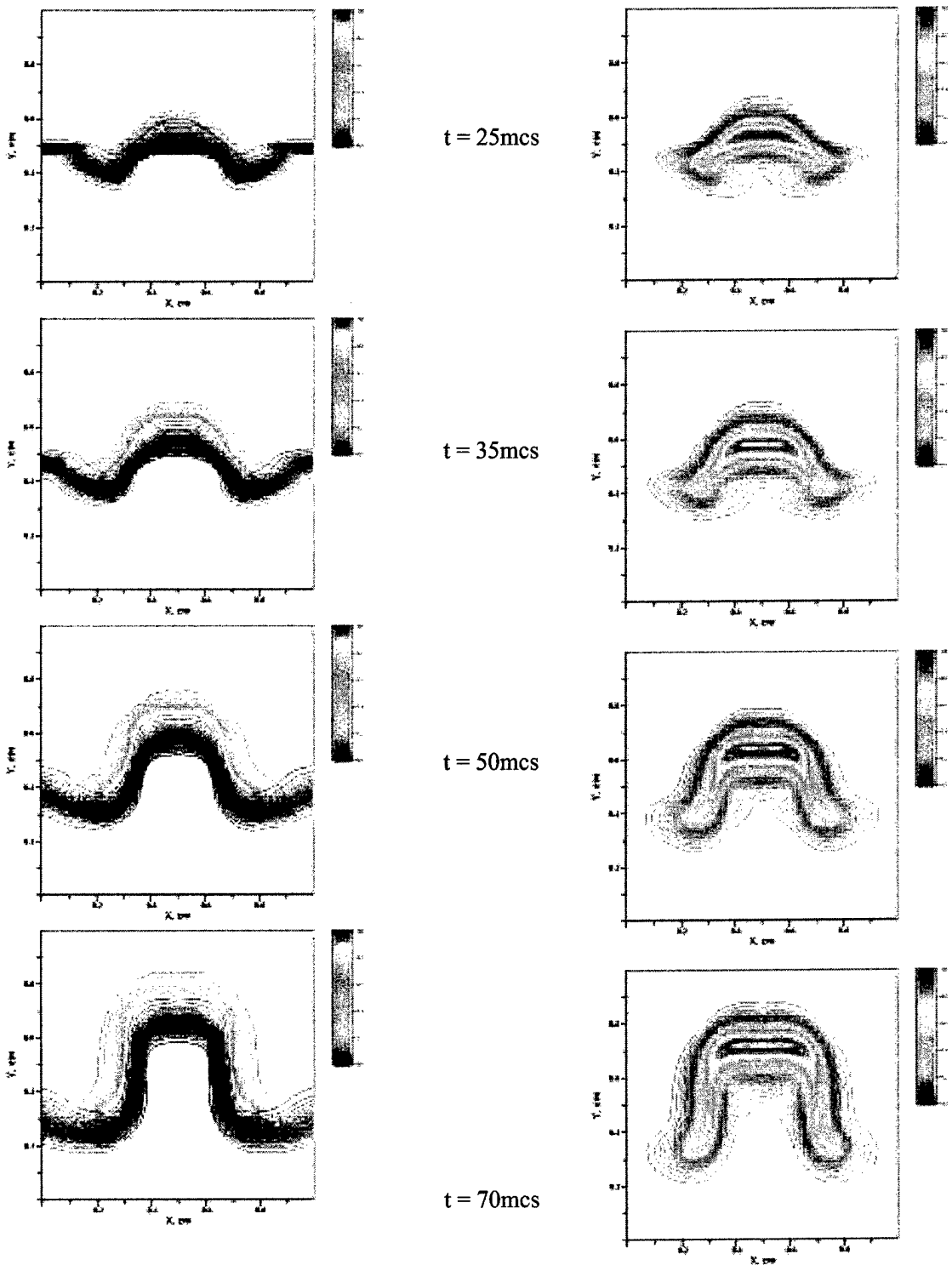

Fig.3. The mass fractions of hydrogen and water(left) and temperature(right) for Case 1

The Fig.3 represents the process of MHD driven mixing and ignition. The result has been obtained with full numerical model described in the previous Part II. The model includes 2Dt simulation of the reacting gases with accounting of diffusion, heat conductance and viscosity effects. The chemical kinetics scheme used has been also described in the previous Part. This scheme describes the combustion of hydrogen in air on the base of a simplified scheme consisting of 42 reactions with nine species involved. Nitrogen is considered as a passive component considered as a third body molecule. At this stage no ions chemistry has been included. Thus, the results obtained in this simulation should be considered as qualitative.

In the left column of Fig.3 the weight fraction of the hydrogen and water – main final product of the combustion are presented. The hydrogen concentration level lines (dark monocolor lines) indicated the diffusion region where the hydrogen fraction differs from 1 (the initial value in a lower part of the domain). Due o rather low temperature in gas surrounding the arc the rate of chemical reaction is negligible low, no combustion is observed in primary diffusion region. In the contrast to this the diffusion region formed at the tip of the arc cross-section moving to the contract surface is heated-up by the energy release in the arc. So the temperature of the mixture here is high enough to initiate the hydrogen oxidation reactions. The water fraction is represented in Fi.3 by colored level lines. It is clearly seen that since the arc approached the interface surface he water production increases rapidly. It is interesting fact that maximum water concentration does no coincide with the maximal temperature location but always behind of that from the hydrogen side.

Future study will be devoted to parametric investigation of such a process of MHD driven ignition.

4. **Experimental Validation Scheme**

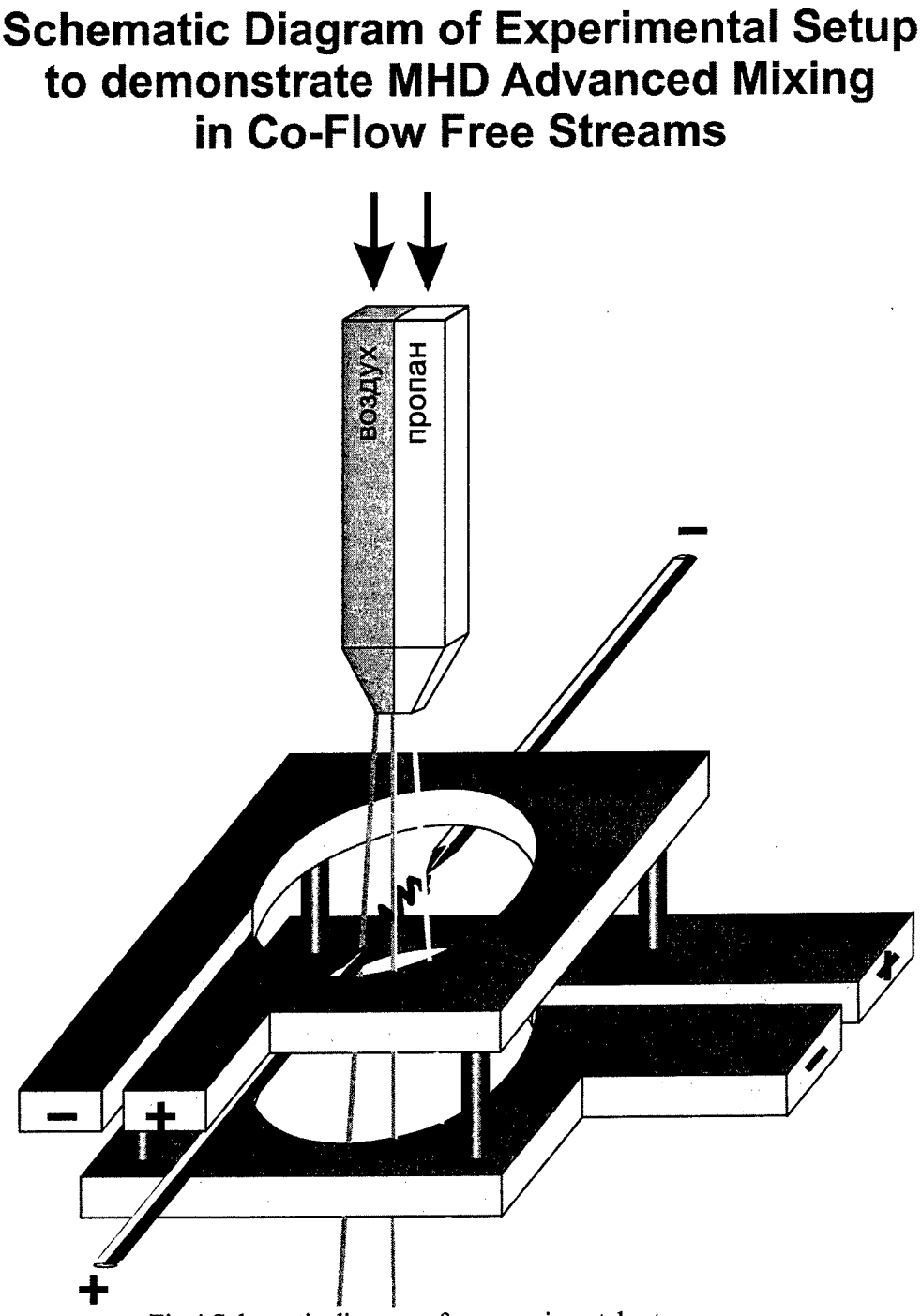

Fig.4 Schematic diagram of an experimental setup

In Fig.4 one of the possible arrangements of small laboratory setup to demonstrate the effect of MHD driven mixing and combustion in co-flow streams is presented. The facility includes two gas sources ('fuel' and 'oxidant'), magnetic induction system, and electrical discharge system. The magnetic filed induced along the main velocity of jets in combination of the arc discharge organized near the contact surface of the two jets create the body force driving the arc channel across the free jets. According the preliminary estimates and numerical simulation such a configuration ca improve the combustion performance significantly.

In more detailed the proposed experimental facility will be described in the Final report of the related project supported by ISTC.

General Conclusion

The new concept of MHD driven Advanced mixing of gaseous fuel-oxidant system in a high-speed combuster are formulated.

The background of such a concept consists of the earlier developed model of kinematics mixing in vortex turbulent flows.

The vortex nature of the Lorentz body force resulting from perpendicular vectors of electrical current and externally applied magnetic filed provides the flow vorticity intensification.

The enhancement of the mixing under such conditions is characterized by an exponential growth of the contact surface square in a turbulent flow.

The second mechanism – molecular diffusion is responsible for the creating the flammable mixture in an physically infinitely small volume.

These two mixing mechanisms are combined to formulate the concept of reacting volume – the volume where only the combustion is possible.

Besides of the qualitative physical model the proper numerical model has been developed to study the process on the microscopic scale.

This model includes the treatment of chemical reacting flows on the base of full Navier-Stockes approach, chemical kinetics model, and MHD effects model.

Preliminary results confirm the basic physical ideas. The combustion in co-flow streams can be effectively initiated and control by the manipulation of he electrical parameters: strength of external magnetic field and electrical discharge current.

The preliminary sketch of the future laboratory scale experiment is presented as well.

The parametric study of the proposed concept as applied to the conditions typical for he practical situation in a scramjet/ ramjet will be completed in a related project supported by ISTC in 2000/2001.

Acknowledgement

This report is based upon work supported by the European Office of Aerospace Research and Development, Air Force Office of Scientific research, Air Force Research Laboratory under Contract SPC 99-4093. the work has been monitored by Dr.S.Walker.

The authors are gratefully acknowledged to EOARD and personally to Dr.C.Raffoul for financial and moral support during the project.

Applications

i. "The Contractor, Dr.Valentin Bityurin, hereby declares that, to the best of his knowledge and belief, the technical data delivered herewith under Contract SPC 99-4093 is complete,accurate, and complies with all requirements of the contract."

ii. "I, the Contractor, Dr.Valentin Bityurin, certify that there were no subject inventions to declare as defined in FAR 52.227-13, during the performance of this contract."

iii. "Any opinions, findings and conclusions or recommendations expressed in this report are those of the authors and do not necessarily reflect the views of any other person and organizations."

DATE:_____ September 30, 2000.

Name and Title of Authorized Official:
Valentin A. BITYURIN, PhD,DS
Contractor _____

References

1. Я.Б.Зельдович. Теория горения и детонации газов. М., Изд-во АН СССР, 1944.
2. Д.А.Франк-Каменецкий. Диффузия и теплопередача в химической кинетике. М.,Наука, 1987, 502 с.
3. F.A.Williams. Combustion Theory, Benjamin Cummings, 1985.
4. P.A.Libby and F.A.Williams. Turbulent Reacting Flows, Academic Press, 1994.
5. V.R.Kuznetsov and V.A.Sabel'nikov. Turbulence and Combustion, Hemisphere publishing corporation, English edition, 1990.
6. Valery Morgenthaler, Lufs Fernando Figueira da Silva, Bruno Deshaies, Vladimir A.Sabel'nikov. Non-Premixed Combustion in Supersonic Turbulent Flows: a Numerical Study for Co-flowing H2-Air Jets, AIAA 99-4917, 9th Intern. Space Planes Hypersonic Systems and technologies Conference, November 1-4, 1999/Norfolk, VA.
7. 1999 Contractors' Meeting in Chemical Propulsion, Holiday Inn Sunspree resort, Bar Harbor, ME, 13-16 June 1999
8. J.M.Ottino. The kinematics of mixing: stretching, chaos, and transport. Cambridge University Press, 1997.
9. В.А.Битюрин, В.Г.Потебня, А.Л.Цескис, Об эволюции токонесущего плазменного сгустка в среде со случайным полем скоростей // Письма в ЖТФ, 1996, т.22, №2, с.80-83.
10. В.А.Битюрин, В.Г.Потебня, А.Л.Цескис, Перенос энергии в газоплазменном течении при наличии токопроводящих кластеров. // Магнитная гидродинамика, 1997, т.33, №3, с.297-305.
11. V.A.Bityurin, V.G.Potebnya, A.L.Tseskis, V.A.Bityurin, V.G.Potebnia and A.L.Tseskis. Evolution of a Current Plasma Clot in Turbulent Flow. Proc. Of 33rd SEAM Conf., Tennessee, June 12-15, 1995, p.IV.7.
12. V.A.Bityurin, V.G.Potebnya, A.L.Tseskis,
13. V.A.Bityurin, A.N.Bocharov, V.G.Potebnya, N.Yu.Babaeva, V.G.Naidis, A.L.Tseskis, Modeling of Processes in GCB around Current Zero, IVTAN – ANRA, June 1999.
14. . G.K.Batchelor. Proc.Poy.Soc.A213, 1114, p.349-366.
15. Monin D.S., and Jaglom A.M. Statistical Hydro-mechanics. Mechanics of Turbulence. Part I. // M., «Nauka», 1965, 639 p. (in Russian).(See also: A.S.Monin and A.M.Yaglom. *Statistical Fluid Mechanics*, v.1, Pergamon, 1965.)

16. Monin D.S., and Jaglom A.M. Statistical Hydro-mechanics. Mechanics of Turbulence. Part II. // M., «Nauka», 1965, 670 p. (in Russian).(See also: A.S.Monin and A.M.Yaglom. *Statistical Fluid Mechanics*, v.2, Pergamon, 1965.)
17. L.D. Landau and E.M. Lifshits. *Hydrodynamics*, M., Nauka, 1988, 733 p., (in Russian).
18. R.Rosa. *Magnetohydrodynamics Energy Conversion*, M., MIR, 1970, 288 p., (in Russian).
19. H.Schlichting, Grenzchicht-Theorie. Verlag G.Braun. Karlsruhe, 1951.
20. W.H.Reid. Proc.Camb.Phil.Soc.51, 2, p.350-362.